Review

Information, Geometry, and Chaos: Revealing Latent Cysteine Butterflies on Fractal Redox Shapes in the Proteomic Spectra

James N. Cobley *

Posted Date: 25 July 2025

doi: 10.20944/preprints202507.2120.v1

Keywords: cysteine; redox; proteomics; information; chaos; proteoform

 doi:10.20944/preprints202507.2120.v1

Review

Information, Geometry, and Chaos: Revealing Latent Cysteine Butterflies on Fractal Redox Shapes in the Proteomic Spectra

James N. Cobley

The School of Life Sciences, The University of Dundee, Dundee, DD1 5EH, Scotland, UK;
jcobley001@dundee.ac.uk or j_cobley@yahoo.com

Abstract

Reversible cysteine oxidation is a central mechanism of protein regulation, commonly studied through advanced redox proteomic workflows that systematically catalogue the redox state of thousands of residues. Excitingly, these expansive datasets contain latent information that remains largely untapped. In this work, we propose that principles from information theory, signal geometry, and chaos theory can reveal hidden meaning within these data—illuminating dynamic regulation, molecular memory, and the interplay between order and chaos in redox biology. Drawing on concepts such as Shannon entropy, Fisher information, and spectral energy, we show how variability and spread in redox signals may reflect structured, condition-specific differences rather than random noise. We further define a mathematical basis for a cysteine redox butterfly effect on fractal redox manifolds where sensitivity to initial conditions produces chaotic responses. Even simple entropy-based metrics can uncover coherent patterns in existing datasets, motivating a conceptual shift in how redox proteomic data can analyzed and interpreted. We further propose that oxidation can be viewed as a probabilistic signal field shaped by underlying biochemical, spatial, and evolutionary constraints. This reframing opens new avenues for extracting insight from existing data and offers a conceptual bridge toward future models of redox biology.

Keywords: cysteine; redox; proteomics; information; chaos; proteoform

1. Introduction

Reversible cysteine residue oxidation redox-regulates biological processes by dynamically modifying protein structure and function [1]. These oxidative post-translational modifications (PTMs [2–6]) influence protein activity, stability, localization, interactions, and phase [7]—making cysteine oxidation a powerful and versatile mechanism of cellular control [8]. Viewed from a systems perspective, redox regulation operates like an electrical circuit: the sulfur atom in cysteine functions as a live node, continuously reshaped by the flux of oxidizing and reducing equivalents [9]. This nodal flux is modulated by a metabolically wired redox module comprising oxidants—reactive oxygen species (ROS) like hydrogen peroxide (H_2O_2)—and reductants, including the glutathione (GSH) and thioredoxin (Trx) systems [10–12].

As reviewed elsewhere [13–17], mass spectrometry-based redox proteomics enables a systems-level readout of this biochemical circuitry by quantifying the percentage oxidation of individual cysteine residues across the proteome [18–25]. These residue-resolved oxidation states provide a relative, condition-specific map of electron flux throughout the networked circuit [26]—offering a powerful lens through which to observe the dynamic output of the upstream redox module [27]. These redox proteomic approaches have yielded important insights into signaling pathways [28], stress responses [29], aging [18], immunity [30], and disease mechanisms [31]—each shaped by the underlying flux of oxidants and reductants [32].

 doi:10.20944/preprints202507.2120.v1

Current redox proteomic frameworks largely treat the redox state of each residue as a vector with direction and magnitude. These residue-level vectors enable condition-specific changes to be analyzed using standard approaches, such as volcano plots. Excitingly, the power of such analyses can be amplified by considering the latent information encoded by the ensemble of vectors as a whole. This holistic perspective can reveal emergent structure, function, and circuit-level output—features of the redox system that may remain hidden when residues are considered in isolation. For example, high-dimensional analyses can provide transformative insights—like ordered and chaotic cysteine redox state patterns—that may already be latent features in extant datasets [27].

To reveal latent features, the present review focuses on the analysis and the reinterpretation of redox proteomic datasets using high-dimensional, information theory-grounded metrics like Shannon entropy [33]. Since the underlying redox biology and proteomic technologies have been comprehensively reviewed [34–48], we begin by defining how redox proteomic data are currently analyzed and interpreted. We then introduce a set of information-theoretic tools for high-dimensional analysis and demonstrate how these concepts can uncover emergent features—including structure, symmetry, and chaos [49]. These emergent features enable peptide-centric proteomics to better describe cysteine proteoform defined bioelectrical circuits [50]. What follows is a new way of thinking and speaking about redox biology. It is a language grounded in the grammar of information theory, shaped by chaos, and expressed through dynamic nonlinear systems.

2. The Flatland Problem: How Scalar Redox Values Conceal the High-Dimensional Structure of Peptide Data

2.1. Setting the Stage: Conventional Approaches to Analyzing Redox Proteomic Data

Redox proteomic datasets usually comprise redox state vectors encoding the direction and magnitude of a given state in the percentage basis—from 0 to 100% oxidized—for thousands of cysteine residues across one or more conditions [18,51–59]. Typically, these vectors arise from the spectral measurement of peptide ensembles bearing light (reduced) and heavy (reversibly oxidized) labels—such as isotopically distinct maleimide probes [25,60,61]—at both the MS^1 (intact peptide) and MS^2 (fragment ion) levels [62–67]. Each spectral "read" is therefore an amalgam of binary 0 and 1 intensities—corresponding to light and heavy modified peptides and their fragments—that collectively encode the overall signal for a given peptide. These signals are usually converted into percentages following the processing of the raw files using appropriate software like MaxQuant or DIA-NN for data-dependent acquisition (DDA) and data-independent acquisition (DIA) schemes, respectively [68–70].

Most current frameworks treat the residue-level redox state as a scalar datapoint—a single numerical value encoding the degree of oxidation—to enable rigorous statistical comparisons between conditions. Each scalar is treated as a scale-bounded continuous variable, capable of assuming any real value within the closed interval [0, 100] [71,72]. These data are typically analyzed by comparing scalar values between conditions using appropriate statistical tests, such as independent t-tests for parametric datasets, with corrections applied to control for family-wise error rates. A common visualization method is the volcano plot, in which the mean oxidation difference (the delta change) between conditions is plotted as the $\log_2$ fold-change against a significance metric, such as the $-\log_{10}$ adjusted *P*-value. This approach captures both the magnitude and direction of redox shifts and is particularly useful for identifying cysteine residues with significant, condition-specific perturbations—for instance, in age-associated redox stress response [73–77].

To extract broader biological patterns from the scalar redox data, many studies apply dimensionality reduction techniques, such as **Principal Component Analysis (PCA)** [78]. PCA transforms the original high-dimensional dataset—where each residue is a variable—into a reduced set of orthogonal axes (principal components) that capture the greatest variance in the data. This enables the visualization of global structure, such as sample clustering by condition, tissue, or genotype, while preserving the most informative variation. In parallel, **unsupervised clustering**

 doi:10.20944/preprints202507.2120.v1

algorithms—such as hierarchical clustering or k-means—are often used to group residues or samples based on shared redox patterns [27]. These approaches can reveal context-specific clusters, like tissue-specific oxidation signatures [18,79], helping to identify coherent redox modules across biological systems [80,81]. Together, PCA and clustering extend scalar analysis beyond univariate comparisons by revealing coarse-grained structure in the data, forming a conceptual bridge between single-site analysis and more integrated, systems-level insights.

2.2. The Flatland Problem: The Limitations of Scalar, Linear Analyses

While **scalar-based approaches enable powerful statistical analyses, they also impose a reductionist structure that can obscure biological meaning, which we term the "flatland problem".**

By treating each cysteine residue as an independent variable, these methods flatten the system into a residue-centric view, fragmenting the natural continuity of protein-level redox behavior. This flat projection into low-dimensional space disrupts the coordinated structure of the underlying redox manifold. In this manifold, each residue belongs to a specific **cysteine proteoform**—a defined molecular configuration determined by the redox state of all cysteines in that protein molecule [50]. Hence, clusters or components derived from conventional analyses reflect statistical groupings of residues, not coherent **proteoform dynamics**. This disconnect matters: it is proteoforms—not their disembodied peptides—that enact biology [82–86]. Redox regulation is not merely a collection of residue shifts [87], but a coordinated molecular choreography that scalar analysis cannot fully resolve [88–90].

While peptide-level oxidation percentages appear continuous, they are ensemble averages over **discrete molecular states** [91–95]. For example, a protein molecule with three cysteines can exist only in one of four possible proteoform oxidation modes: 0%, 33%, 66%, or 100% [27,50,87,96,97]. However, what we measure is a peptide-level readout—an aggregate signal reflecting a distribution over these unseen modes [98]. Linear models treat this data as continuous, but the originating system is fundamentally discrete and combination constrained.

The tension—between continuous analysis and discrete biological configuration—reveals a core limitation of current frameworks. It invites new models that acknowledge the **latent structure of cysteine proteoforms embedded in high-dimensional state space** [96,99].While these proteoforms are not directly observed in bottom-up mass spectrometry [100–102], peptide measurements are projections of their redox state distributions. Hence, methods that recognize this structured embedding are better equipped to recover the coordinated, nonlinear behavior of redox systems [103–105].

2.3. Embracing High-Dimensional Complexity

Nonlinear models can be directly applied to peptide-level oxidation data [106]. Nonlinear models are sensitive to **thresholds, feedback loops, bifurcations, and emergent behaviors** [49,97,107]. For example, a small change in oxidation at one cysteine may lead to a disproportionate structural or functional shift in the protein, particularly if it triggers allosteric change or destabilizes a critical motif [108–111]. Even without measuring cysteine proteoforms [87], nonlinear models applied to peptide data can uncover signatures of **non-additivity** and **non-monotonicity** in redox behavior. These models can help to recover the logic of the system: a redox landscape not governed by smooth gradients but by **discrete jumps, state transitions**, and **multi-stable basins of behavior** [112].

Zooming out, we cast the behavior of the networked redox circuit in a new light by considering the language of both information and chaos theory. These theories provide a rich, and mathematically rigorous way of describing the redox dynamics. They can uncover novel features of redox state changes that are already potentially embedded in the peptide-level datasets. We use the term "redox state changes" to be mathematically faithful to the source data devoid of context-specific positive or negative connotations. The scalar oxidation values defining these state changes currently define

 doi:10.20944/preprints202507.2120.v1

flattened projections of a richer, structure that may be revealed through the lens of nonlinear dynamical systems.

3. Information and Chaos Theory: A Framework for Redox Proteomics

3.1. Conceptual Foundations

When seeking to quantify the uncertainty or structure within a signal, **Claude Shannon's 1948 masterpiece** [33] introduced a new mathematical framework now known as *information theory*. Shannon's goal was to formalize the process of communication—how to transmit messages over noisy channels with maximal efficiency and minimal error. He defined informational *entropy* as the average uncertainty or surprise associated with a set of outcomes. The resulting entropy was not about the second law of thermodynamics, but about the number of choices available—the informational richness of a distribution of datapoints in the discrete binary basis [113].

In transcending telecommunications, information theory permeated virtually every branch of scientific study, including biology [114–116]. It now provides a general language for quantifying structure, uncertainty, redundancy, and complexity in diverse systems—from neural networks and genetic sequences to language, learning, and thermodynamics. Central concepts such as mutual information, Kullback–Leibler divergence, and algorithmic complexity enable precise descriptions of how patterns emerge, propagate, and are constrained by prior states. This naturally intersects with **Bayesian inference** [117], which formalizes how prior knowledge influences probabilistic updates in light of new data. In essence, information theory reveals how order and unpredictability are balanced within any probabilistic system, making it a natural partner to dynamical frameworks like chaos theory that explore how such systems evolve over time [118].

While modeling atmospheric convection in the early 1960's, Edward Lorenz discovered that even deterministic systems could behave unpredictably [119]. His seemingly minor rounding error in initial conditions led to radically different weather simulations—an observation that inspired **chaos theory** [120]. Lorenz's insight revealed that **nonlinear dynamical systems**, though governed by deterministic rules, could exhibit **sensitive dependence on initial conditions**—the "butterfly effect" [121]. This realization catalyzed the development of advanced mathematical frameworks—including **strange attractors, Lyapunov exponents,** and **fractals**—to characterize the intricate, self-similar, and often beautiful structures underlying complex dynamical behavior [122–124].

As elaborated herein, information and chaos theory provide a rigorous mathematical foundation for analyzing redox data in fundamentally new ways—redefining how we interpret cysteine redox state changes.

3.2. Shannon Entropy: Quantifying Uncertainty in Redox Distributions

Let the redox proteomic dataset be discretized into percentage oxidized bins, where each bin defines a given range of peptide oxidation values. For example, 50, 2%-oxidized bins over the [0,100] interval. Let p_i be the proportion of peptide datapoints falling within bin i, such that the sum of all bins equals 1. Then Shannon entropy (H) becomes:

$$H = -\sum_{i=1}^{n} p_i log_2 P_i$$

By binning the redox state into discrete intervals, the continuous oxidation data are converted into a valid probability distribution which is mathematically justified because Shannon entropy is defined over discrete outcome spaces. Biologically, the bins correspond to semantically meaningful states (e.g., 100%-reduced [125–127]). The range of each bin can be adjusted depending on the nature of the experiment.

Applied to redox proteomics, Shannon entropy quantifies the **distribution of information**—that is, how redox values are spread across discrete oxidation bins (**Figure 1**). A **uniform distribution** corresponds to maximal entropy, indicating maximal uncertainty or randomness in the oxidation

 doi:10.20944/preprints202507.2120.v1

state data. In contrast, a **sharp peak localized to a single bin** implies minimal entropy—high predictability and low diversity in cysteine redox states. Geometrically, entropy reflects the distribution shape: a flat plateau suggests maximal uncertainty, while a narrow spike reveals an ordered, constrained system.

While the dataset can be addressed globally, Shannon entropy can also be computed **per protein**, **per pathway**, or **per subcellular compartment**—any level where oxidation measurements exist [23]. In this sense, entropy becomes a **local or system-wide lens**, capable of revealing whether the cysteine redox state changes are **dispersed, focused, or compartmentalized** across biological hierarchies. This flexibility can capture the information structure embedded within complex, high-dimensional redox proteomic landscape [128–130].

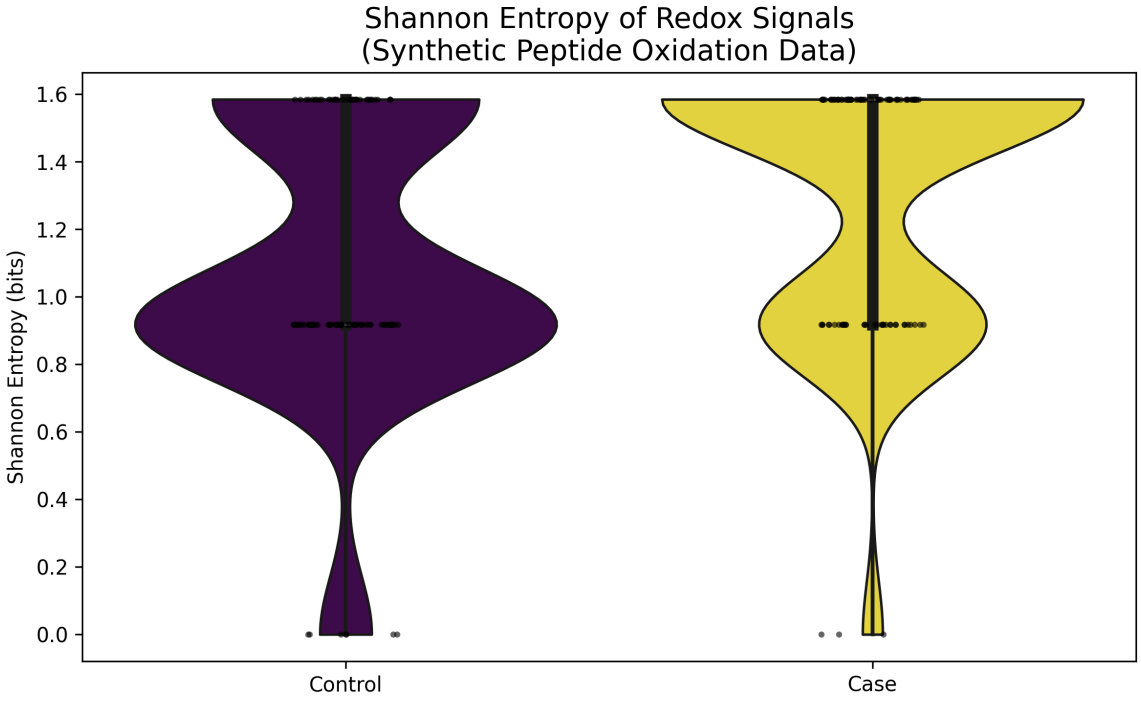

Figure 1. Shannon entropy of redox signals reveals distinct oxidation information profiles between control and case conditions. Synthetic peptide oxidation data were used to simulate redox state distributions under control and perturbed (case) conditions. Shannon entropy was computed for each peptide based on the distribution of its oxidation states. Violin plots display the full distribution of entropy values (in bits) across 100 peptides per group. Control peptides exhibit a bimodal entropy distribution, with dominant populations near 0.92 and 1.58 bits, reflecting discrete or highly structured redox states. In contrast, case peptides show a compressed entropy profile with a peak near maximal entropy, suggesting increased disorder or a broader mix of oxidation states. This visualization highlights the ability of Shannon entropy to quantify redox state variability and infer underlying regulatory dynamics. Figure 1 was generated in google colab using a python script and data that is available at https://github.com/JamesCobley/Redox_information.

3.3. Kullback-Liebler Divergence: Quantifying the Geometric Difference Between Redox State Distributions in Information Space

Let redox proteomic data from two conditions like control and H_2O_2-treated [131] be discretized into the same percentage-oxidized bins, such that $P = \{P_i\}$ represents the baseline condition (e.g., control) and $Q = \{Q_i\}$ represents the perturbed state (e.g., H_2O_2). Each P_i and Q_i denotes the proportion of peptides falling into bin i, normalized such that $\sum P_i = \sum Q_i = 1$. The **Kullback-Leibler (KL) divergence** from Q to P is defined as:

$$D_{KL}(P \parallel Q) = \sum_{i=1}^{n} p_i log_2 \left(\frac{p_i}{q_i}\right)$$

 doi:10.20944/preprints202507.2120.v1

This equation formalizes the **informational cost** of assuming distribution Q compared to P. KL divergence captures how much the cysteine redox state has changed across the full distributional structure.

Applied to redox proteomics, KL divergence can quantify how much information is gained (or lost) when the system is perturbed (**Figure 2**). A low KL divergence suggests minimal redistribution of oxidized peptides, whereas a high value signals substantial reorganization—emergent oxidation peaks, redistribution across bins, or bimodality. Bimodality defining a distribution across two distinct peaks. Geometrically, KL divergence measures how one probability distribution shape differs from another in information space. Unlike Euclidean distance, it is asymmetric $D_{KL}(P \parallel Q) \neq D_{KL}(Q \parallel P)$, preserving the temporal or causal directionality of cysteine redox state changes.

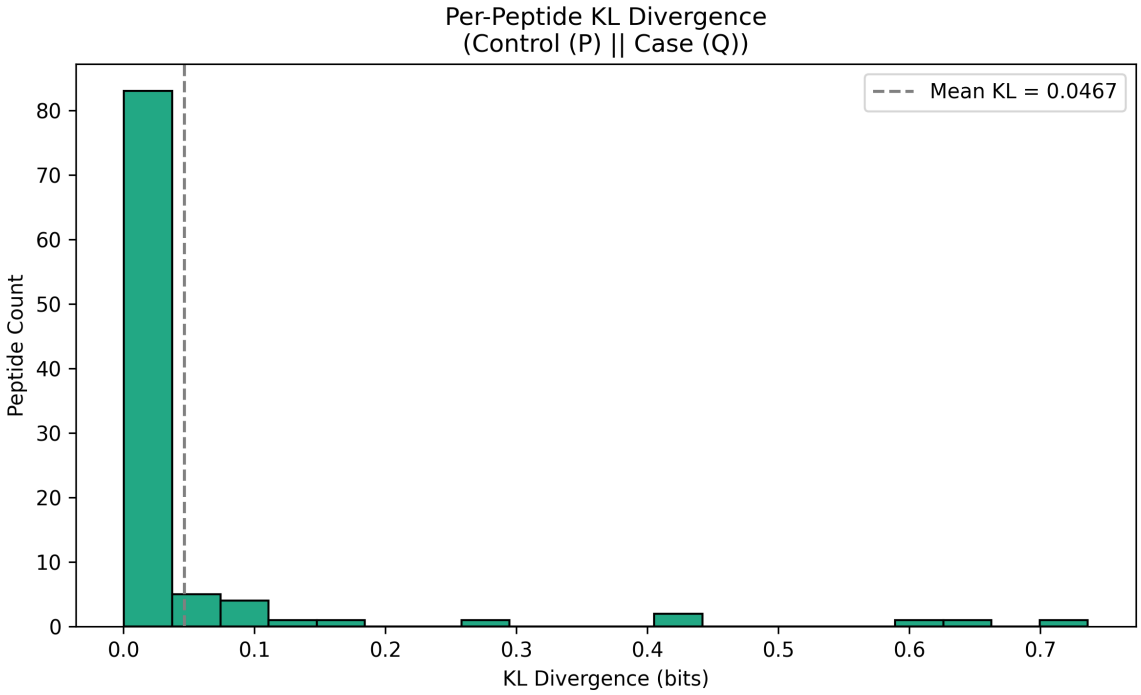

Figure 2. ***Distribution of per-peptide Kullback–Leibler (KL) divergence between control and oxidant-treated conditions***. Each peptide's oxidation probability distribution (P: control; Q: case) was discretized into equal bins and KL divergence $D_{KL}(P//Q)$ was calculated in bits. Most peptides exhibit minimal divergence, suggesting stable redox profiles, while a subset shows substantial shifts under perturbation. The dashed line indicates the mean KL divergence across all peptides (0.0467 bits), quantifying the average informational cost of assuming the perturbed state distribution given the baseline. Figure 2 was generated in google colab using a python script and data that is available at https://github.com/JamesCobley/Redox_information.

Like Shannon entropy, the KL divergence can be applied to multiple biological levels—globally across the proteome, or restricted to peptides from a single protein or pathway—making it a versatile and scalable metric.

3.4. Fisher Information Metric: Quantifying the Geometry of Curved Redox State Manifolds

Let the redox peptide oxidation data be characterized by a probability distribution $p(x;\theta)$, where θ is a parameter (or vector of parameters) that defines the shape or structure of the distribution—such as a mean oxidation state across peptides. The **Fisher Information metric (FIM,** $I(\theta)$ quantifies how much information the data carries about this parameter, which can be formalized as:

$$I(\theta) = \mathbb{E}\left[\left(\frac{\delta}{\delta\theta} log, p(\mathrm{x};\theta)\right)2\right]$$

 doi:10.20944/preprints202507.2120.v1

Applied to a given redox proteomics scale, FIM can describe how sharply a system responds to perturbations like exercise [132–140]. For instance, two distributions with the same mean oxidation might differ in how tightly they are concentrated around that mean [141]. Hence, the FIM captures this **second-order structure**—the local curvature of the data landscape (**Figure 3**). Geometrically, the FIM defines a Riemannian geometry on the space of probability distributions. It introduces curvature to the informational manifold: distributions that are more sensitive to parameter shifts lie on steeper, more curved regions, whereas robust or flat distributions lie in shallower area. These redox state data-derived manifolds can be described in terms of geometric distances and angles.

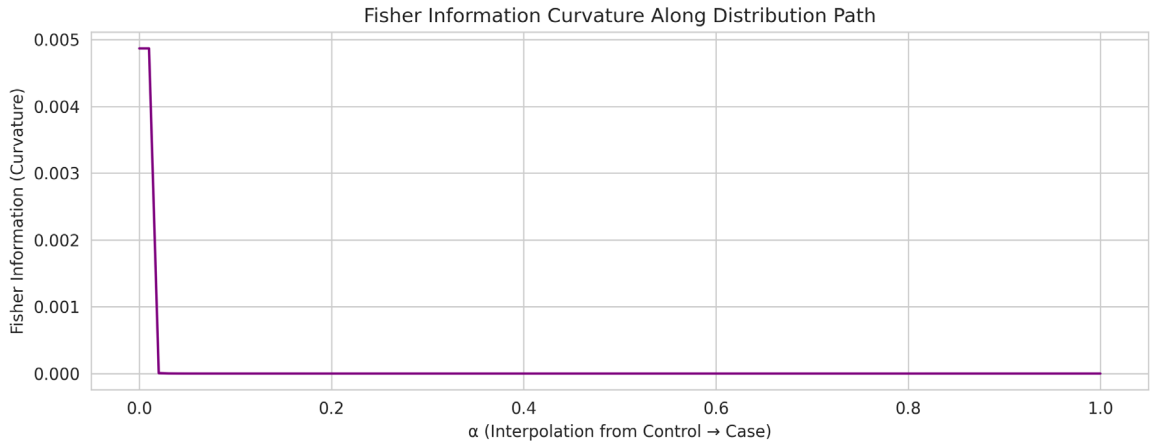

Figure 3. Fisher information curvature reveals sensitivity along the redox state transition path. Fisher information was computed along a continuous interpolation (α) between control and case redox state distributions, where $\alpha = 0$ represents the control condition and $\alpha = 1$ the perturbed case. This analysis quantifies the curvature of the informational manifold traced by the interpolated distributions. A sharp peak in curvature at $\alpha \approx 0$ indicates that the system is most sensitive to changes near the control state, where small perturbations in redox probabilities lead to disproportionately large changes in informational structure. Beyond this region, curvature flattens, suggesting diminished sensitivity and a more stable informational landscape. These results illustrate how Fisher information curvature can detect the nonlinear response profile of redox systems to perturbation, offering a geometric lens on redox state evolution. Figure 3 was generated in google colab using a python script and data that is available at https://github.com/JamesCobley/Redox_information .

Interpretationally, high FIM values might correspond to **tipping points**, where small redox shifts drastically reconfigure the proteomic landscape (e.g., triggering signal response thresholds [142–144]). Conversely, flat regions with low Fisher Information may indicate **robust zones** [145–147], where cysteine redox state changes are dynamically buffered—"homeo-dynamics" [148].

3.5. Fisher-Rao Distance: Quantifying the Distance Between Curved Redox Manifolds

Let the redox peptide oxidation data be characterized by a probability distribution $p(x;\theta)$, where θ parameterizes a family of redox states. While the FIM describes the local curvature around a single distribution, the **Fisher–Rao distance** (d_{FR}) measures the true path length between two such distributions on the curved statistical manifold. Formally, this geodesic—the shortest path length—distance is defined as:

$$d_{FR}(\theta_1, \theta_2) = \int_{\theta_2}^{\theta_1} \sqrt{I(\theta)\delta\theta}$$

Applied to redox proteomics, Fisher–Rao distance defines the true informational displacement between redox states—accounting not just for the magnitude of redox change, but for how the **statistical curvature** of the system warps that change. Two distributions might appear close in Euclidean metrics, yet lie far apart on the information manifold if one lies in a steep, sensitive region and the other in a flat, buffered one. Geometrically, the Fisher–Rao distance measures the shortest

 doi:10.20944/preprints202507.2120.v1

possible path between redox states while honoring the manifold's internal curvature—akin to walking over a hill instead of cutting through it. This defines the "true" distance between redox states in terms of the system's sensitivity to change—where a greater distance indicates the systems not only differ in their values but their geometry (**Figure 4**).

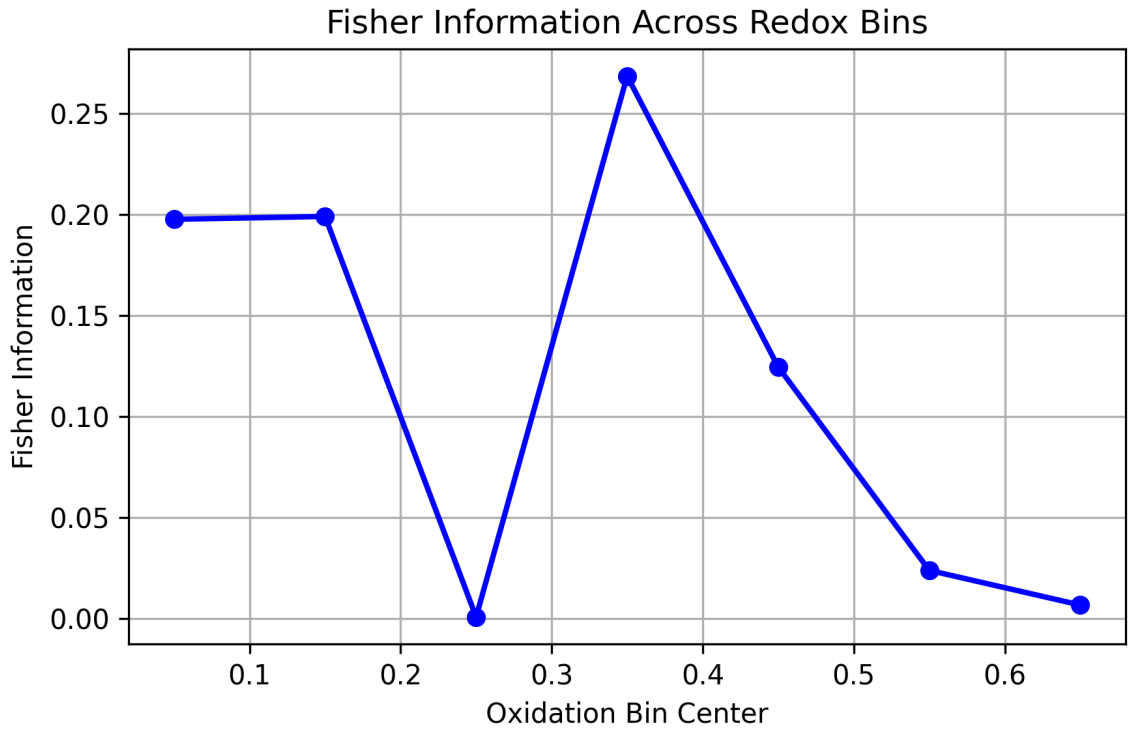

Figure 4. Fisher information across redox bins identifies regions of high sensitivity to redox perturbation. Synthetic peptide oxidation data were used to simulate redox state distributions under control and perturbed (case) conditions. Fisher information was computed across discrete oxidation bins using a symmetric Kullback–Leibler divergence approximation. The resulting curve reveals that specific redox bins exhibit disproportionately high Fisher information—indicating redox regions where small changes in probability carry large informational weight. These high-sensitivity regions may correspond to redox tipping points, regulatory switches, or allosteric thresholds. In contrast, bins with low Fisher information represent buffered or stable oxidation zones with minimal response to perturbation. This analysis highlights the value of Fisher information as a geometric metric for detecting local sensitivity in redox state space. Figure 4 was generated in google colab using a python script and data that is available at https://github.com/JamesCobley/Redox_information .

Interpretationally, large Fisher–Rao distances between conditions (e.g., healthy vs. diseased [149]) may signify **deep structural shifts** in the system. Small Fisher–Rao distances, by contrast, may reflect **smooth adaptation**—a curved, minimal transition within a robust regulatory space.

3.6. Distinguishing Order from Chaos in Time-Resolved Redox Dynamics

Let the redox proteome be measured across a time series—such as sequential timepoints under altered mitochondrial function, circadian cycles, or developmental transitions [150–162]. This temporally resolved data introduces a new analytic axis: **how the system evolves**, not just where it is. The **temporal trajectory** of the cysteine redox state may exhibit patterns that are:

- **Ordered**—following predictable or quasi-linear dynamics.
- **Chaotic**—diverging over time due to small differences in the initial conditions.
- **Hybrid**—a cysteine redox system where orderly and chaotic behaviors coexist either across different subsystems, within different time windows, or as structured chaos near low-dimensional attractors.

 doi:10.20944/preprints202507.2120.v1

Chaos theory provides a mathematical framework to distinguish between these regimes by characterizing the **underlying attractor structure** of the dynamical system (**Figure 5)**. Here, the redox trajectory is treated as an evolving signal in phase space, and we ask: *Does it converge to a stable pattern, cycle through predictable states, or exhibit sensitive dependence on initial conditions?*

To distinguish between these behavioral regimes, we draw from a set of mathematically grounded metrics in nonlinear dynamics. These tools quantify whether redox trajectories evolve stably, diverge chaotically, or settle into structured attractors. These tools capture distinct signatures of complexity: **Lyapunov exponents** quantify divergence of nearby trajectories, **recurrence analysis** detects hidden periodicities and long-range dependencies, **correlation dimension** characterizes the geometry of the underlying attractor, and **bifurcation analysis** reveals phase transitions triggered by small parametric shifts [163–168]. Table 1 summarizes each metric, its mathematical formulation, and its interpretation in the context of peptide-resolved proteomics, such as time-resolved cell cycle or signaling analyses [23,169–171].

Table 1. Summary of key chaos theory metrics, inclusive of the mathematical tool, peptide-level equations, and the biological interpretation.

Metric	Mathematical tool	Equation (peptide level)	Biological interpretation
Lyapunov exponent (λ)	Exponential divergence of nearby trajectories.	$\lambda = lim(t \to \infty)(1/t)In(\|\delta X(t)\|/\|\delta X_o\|)$	Positive values denote redox shifts diverging over time. Negative values denote converging or stable trajectories.
Attractor geometry	Correlation dimension (D_2) via Grassberger-Proaccia algorithm.	$D_2 = lim(\varepsilon \to 0)[logC(\varepsilon)/log\varepsilon]$ $where\ C(\varepsilon)\ is\ the\ corrlation\ sum$	Redox states oscillate about nonlinear basins with fractal, self-similar structure.
Entropy production	Kolmogorov-Sinai (KS) or approximate Entropy (ApEn).	$ApEn(m,r,N) = \Phi\,'\mathrm{m}'\,(\mathrm{r}) - \Phi'\mathrm{m}+1'\,(\mathrm{r})$	The dynamic generation of information reflects continually redox remodeling of the peptide oxidation state.
State recurrence	Recurrence quantification analysis (RQA), Poincaré maps.	$R(i,j) = \ominus\left(\varepsilon - \left\|x_i - x_j\right\|\right)$ Where $\ominus$ is the Heaviside function	Detects long-range memory, hidden periodicity, and/or structured noise in cysteine oxidation datasets
Bifurcation detection	Delay-coordinate bifurcation diagram with control parameter.	$X_{n+1} = f(X_n;\mu)$, scan over μ (e.g., ROS flux)	Can reveal whether small redox changes trigger shape transitions in cysteine oxidation—phase space shifts.
Phase-space remodeling	Delay embedding with topological analysis.	$X_t = [X_t, X_{t-}\tau, X_{t-}2\tau \ldots, X_{t-}(m-^1)\tau] \in \mathbb{R}^m$	Can reveal the stretching and folding that is characteristic of chaotic attractors.

Notes: xt is the cysteine redox state (e.g., %-oxidation) of a given peptide at time t. δX(t) and δX0 are small perturbations in peptide oxidation trajectories. m is embedding dimension; τ is time delay; μ is a control parameter (e.g., ROS flux). The equations can be computed peptide-wise, then aggregated across peptides or protein.

 doi:10.20944/preprints202507.2120.v1

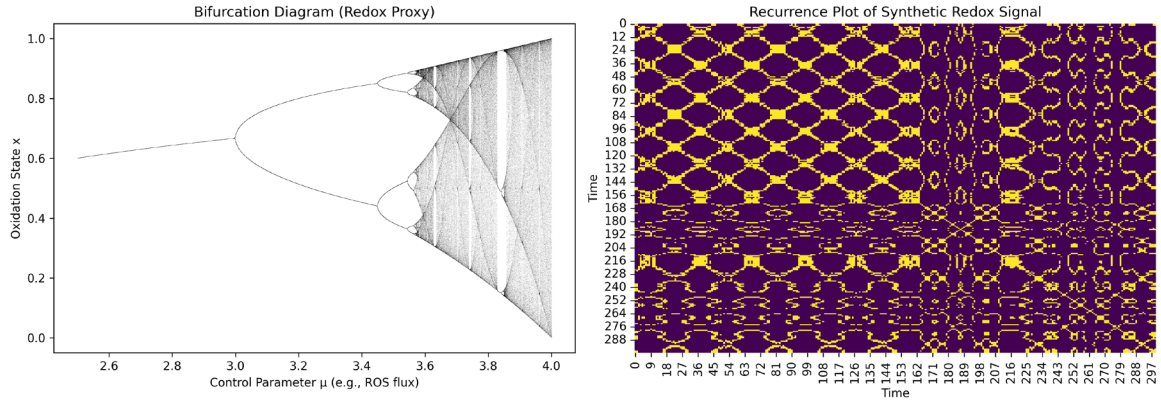

Figure 5. Bifurcation and Recurrence Reveal Emergent Redox Chaos in Synthetic Systems. Left: Bifurcation diagram of a logistic map modeling cysteine oxidation under increasing control parameter (μ), representing external redox input such as ROS flux. The system transitions from a single fixed point (ordered behavior) into periodic oscillations, and ultimately chaotic dynamics as μ increases. These bifurcations emulate how redox systems can exhibit critical transitions where small parameter changes drive disproportionate shifts in the proteoform state distribution. Right: Recurrence plot of a synthetic redox signal over time. The top-left region shows regular, periodic recurrence patterns—indicative of stable or oscillatory redox behavior—whereas the lower-right region becomes irregular and fragmented, reflecting transition to chaos. This transition captures the coexistence of order and disorder, consistent with redox hybrid attractors. Such plots reveal hidden periodicity, long-range memory, and the emergence of structured noise within redox trajectories, supporting the concept of "strange oxi-attractors". Figure 5 was generated in google colab using a python script available at https://github.com/JamesCobley/Redox_information.

At the peptide level, these tools allow us to treat nonlinear cysteine redox dynamics as an evolving informational signal trajectory in a high-dimensional state space [97]. These signal trajectories can fold and stretch like a shape being continually remodeled. The resulting shapes—patterns—can exhibit instability and a memory. These measures offer a generative map of how redox perturbations propagate, whether they resolve into ordered recovery or spiral into new basin attractors, which we term **strange oxi-attractors**.

*S*mall differences in initial cysteine oxidation states can cascade into dramatically different outcomes. A minute shift in oxidation at a specific site—triggered by the upstream redox module [172–174]—may push the system across a bifurcation point or into a new attractor basin—a dissipative structure: the strange oxi-attractor [175].

We define this phenomenon as the **cysteine redox butterfly effect. This effect captures the sensitive dependence to initial conditions in nonlinear systems, which while manifest at the proteoform level can be recorded in the redox states of peptides. The cysteine redox butterfly effect** explains how noise can become a biological signal—how tiny molecular events can influence fate decisions, stress responses, or pathogenesis [176–186]. And critically, these changes are not arbitrary. Hence, cysteine oxidation encodes not only the current biochemical state—but the memory of its perturbation history, fractally embedded in time.

3.7. Fractal Geometry: Quantifying Scale-invariant Self-similar Cysteine Redox State Patterns

Let a peptide level cysteine redox trajectory be conceptualized as a curve evolving in complex space, where each peptide's oxidation state is modeled not as a scalar value but as a complex number:

$$Z(t) = R(t) + iI(t)$$

In this formalism, $R(t) \in \mathbb{R}$ **is the real measured percentage oxidation of the peptide at time** t**, and** $I(t) \in \mathbb{R}$ **is an imaginary component, capturing a latent structure, such as the velocity of the redox state change, the geometry (e.g., Fisher-Rao distance), or a measure of entropy (e.g., approximate entropy or Shannon entropy). This transformation lifts peptide-coded cysteine redox**

 doi:10.20944/preprints202507.2120.v1

dynamics into the complex plane ($\mathbb{C}_{Redox}$), where the trajectories—paths in phase space [0,100]—can generate fractals.

Pioneered by Benoit Mandelbrot [123,124,167,187,188], fractals are geometric structures that exhibit **self-similarity across scales**, often governed by recursive rules or nested feedback. Applied to redox proteomics, fractal analysis asks: *Does the oxidation trajectory of a peptide encode recursive or scale-invariant patterns? Do certain biochemical systems evolve along a fractal manifold in redox space?* **To help answer these questions, Table 2 defines** a set of mathematically grounded tools for extracting fractal structure from complex-valued peptide oxidation trajectories. **Figure 6** illustrates a synthetic example of a complex-valued redox signal and its recurrence structure, visually revealing fractal and recursive motifs in $\mathbb{C}_{Redox}$.

Table 2. Mathematically grounded tools for fractal analysis in peptide level redox biology.

Metric	Mathematical tool	Equation (peptide level)	Biological interpretation
Box-Counting Dimension ($D_{(B)}$)	Estimates geometric complexity by covering the trajectory in ε-sized boxes.	$D_B = lim_{\varepsilon \to 0} \frac{log\ N\ (\varepsilon)}{log(1/\varepsilon)}$	Measures how fully the redox trajectory fills its phase space. A High D_B suggests a recursive filling of the available space—the [0,100] interval.
Curvature entropy	Quantifies the entropy (S) of trajectory curvature fluctuations.	$S_{curve} = -\sum_i p(k_i) log p(k_i)$ Where k_i is local curvature.	Measures dynamic inflections in redox trajectories—capturing looping, spiraling, or sharp transition behavior.
Fractal recurrence score	Assesses self-similarity in recurrence plots.	Diagonal line structures in 2D recurrence plots of $Z(t)$; compute fractal dimension of recurrences.	Measures multi-scale repetition in cysteine oxidation patterns, with the ability to capture periodic cycles.
Spectral fractality	Power-law scaling of the trajectory frequency domain.	Power spectrum $P(f) \sim f^{-\beta}$, where $\beta \in (0,2)$ quantifies long-range memory	Measures cysteine oxidation dynamics across timescales with the ability to capture nested cycles or autocorrelation behavior.

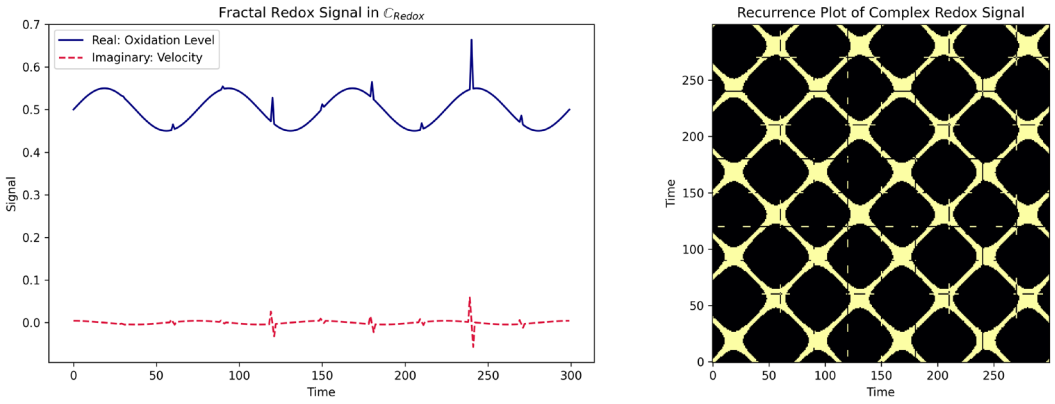

Figure 6. Synthetic fractal redox signal in complex redox space $\mathbb{C}_{Redox}$ reveals scale-invariant recurrence structure. Left. Real component (solid blue) represents the synthetic oxidation level R(t)R(t)R(t) over time. Imaginary component (dashed red) encodes a latent redox variable, here modelled as the temporal derivative of oxidation (velocity), forming a complex signal $Z(t) = R(t) + iI(t)$**.** Periodic base structure with superimposed fractal spikes reflects recursive oxidation dynamics and perturbation events. (Right) Recurrence plot of the

 doi:10.20944/preprints202507.2120.v1

complex signal *Z(t)*, showing repeated trajectory motifs in phase space. The plot reveals nested lattice-like structures with cross-scale diagonals and loops, consistent with a self-similar and fractal manifold in redox space. These patterns suggest memory-like dynamics, attractor basins, and long-range temporal correlations within the redox signal evolution. Figure 6 was generated in google colab using a python script available at https://github.com/JamesCobley/Redox_information.

These metrics may be applied on a per-peptide basis or aggregated across peptides or pathways to infer system-wide fractal signatures. These analyses may also be constrained within specific **time windows** to isolate localized self-similarity.

Interpretationally, fractal geometry can reveal if and how cysteine oxidation patterns recur, nest, or stretch over time. A residue signal with a non-integer fractal dimensional value $D_B \in (1,2)$, suggests scale-invariant, and recursive redox dynamics, like a recurrent oxidation-reduction control cycle gravitating around a basin attractor. The imaginary component in the $\mathbb{C}_{Redox}$ **expression, provides analytical flexibility. It can encode temporal derivatives, conformational entropy, of redox flux sensitivity. As a result, fractal patterns that spiral inward or explode outward can be produced. Fractal geometry can reveal whether the system or aspects thereof exhibits chaotic behavior about strange oxi-attractors via the analysis of fractal redox manifolds.**

We define a fractal redox manifold as a recursive geometric space where peptide oxidation states evolve nonlinearly in a conserved self-similar manner. These manifolds may embody a memory of redox history.

4. Synthesizing A New Framework for Analyzing and Interpreting Redox Proteomic Datasets

Ironically, redox biology resists reduction. It defies simple arithmetic. As evidenced by the failure of the original linear rooted free radical theory of aging [189–193], adding or subtracting electrons doesn't yield proportionate cysteine redox state changes. Instead, it can provoke silence or unleash a cascade. Without violating physics, outputs diverge from inputs. *How?* Because the cysteine redox network is not a passive register of electrons. Instead, it is a dynamic, living network. Actively wiring, perpetually rewiring itself by funneling, channeling, dispersing the electron flux across sulfur nodes. This sulfur nodal flux dynamically remodels cysteine proteoforms distributions [27,50,87,96,97,194].

The instantiated now carries a memory. The oxidation state of cysteine—measured via a peptide level read—holds a record of its past that can offer insights even when the proteoform level information is inaccessible. These redox states tell us how now can shape the future. The profound consequence is that divergence from a given state might not be easily reversed by an "antioxidant" [36,38,195–198]. Even if the antioxidant works as intended [37,40,199], simply curtailing further oxidation will not provide the electrons needed to reduce what is already oxidized [132,200].

A core operating logic emerges where the flow of electron dynamically shapes and reshapes the live sulfur nodes of the cysteine proteome. This incessant flow of energy continually generates entropy by reshaping proteoform matter, structuring their nonlinear dynamics. From the relatively simple redox reactions that determine these states change dynamics, emerges complex behavior—hysteresis, order, chaos, and fractals (**Figure 7**). *But, how do we understand this complexity? How do we differentiate between order and chaos? If needed, can we restore order or provoke redox chaos?*

 doi:10.20944/preprints202507.2120.v1

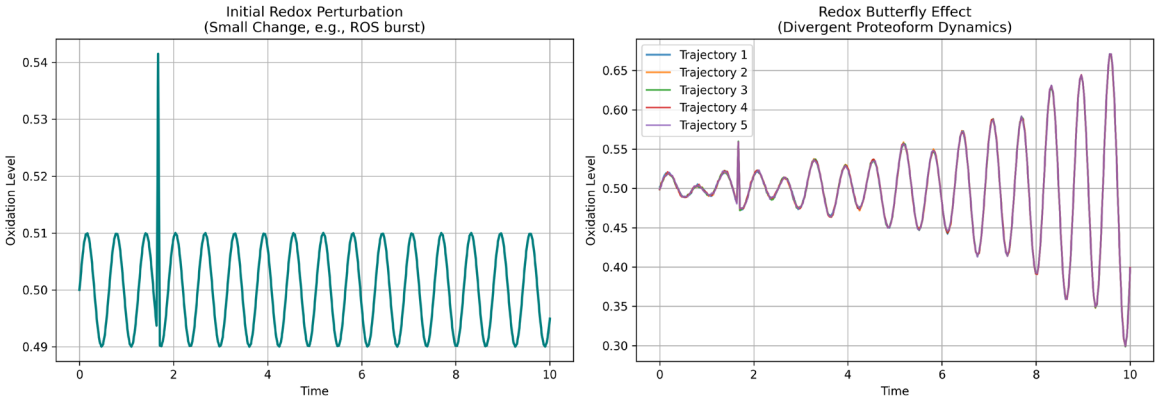

Figure 7. The cysteine redox butterfly effect. A small change in ROS from a redox perturbation (left) provokes chaotic cysteine proteoforms trajectories in redox phase space (right). Figure 7 was generated in google colab using a python script available at https://github.com/JamesCobley/Redox_information.

To better understand the structured signals underpinning complex phenotypes like sleep-loss induced neurodegeneration [201–205], information and chaos theory become indispensable tools for advancing redox proteomic analyses—even when it is peptides not their proteoforms that are measured [206–218].

- **Information theory enables the** oxidation state of a peptide to be analyzed and interpreted as an encoded signal, compressible or not, with measurable entropy. The more irregular, the less compressible—and paradoxically, the more information it may carry. By quantifying these dynamics across timepoints and conditions, one can begin to see that **redox states are not random variables**—they are **deterministic signals with memory**, unfolding on a **nonlinear manifold.**
- **Chaos theory** offers the interpretive lens. Small redox changes can produce outsized shifts in oxidation of peptides. This sensitivity to initial conditions defines the **redox butterfly effect**. Peptide-level oxidation patterns form trajectories—not just in time, but across a **complex redox phase space**, where certain states act as strange oxi-attractor. With tools like approximate entropy, recurrence quantification, and fractal dimension analysis, these structures are now **computationally accessible**, even at the peptide level.

A single oxidation event, once viewed in isolation, can now be seen as part of a larger dynamic system—a ripple in a structured informational field space. Part of a wider cysteine state pattern capable of producing redox fractal manifolds. What began as a measurement of oxidation becomes something else entirely:

A **window into the informational and energetic landscape of the cell**, where peptide-level data carries echoes of phase transitions, stability basins, and bifurcation points.

The dual lens of information and chaos theory can make sense of many anomalies. Like how chaotic attractors in atrial fibrillation demand a shock—not a gentle nudge—to restore rhythm, **redox chaos—or ordered dysregulation—may require a systemic reset.** Any reset is unlikely to stem from the "oxidants bad, antioxidants good" dichotomy [137] as no diseases where "oxidative stress" is implicated have yet been cured along these lines [219]. These disappointing results evidence how much current thinking in redox biology breaks down in the face of nonlinear dynamical systems.

So far, virtually every pharmaceutical redox therapy has fallen short. Perhaps, what's needed is not a molecule, but a mode—a system-wide coherence. These coherent system states may be better achieved not by a "blockbuster antioxidant"—however well-designed—but through basic lifestyle choices. As Barry Halliwell remarked [38], they include sleep, diet, exercise. Each one remodels the energy flowing, matter cycling dynamical logic of the cysteine proteome. For example, exercise induces nuanced reductive and oxidative cysteine redox state changes [138,220–230]. These

 doi:10.20944/preprints202507.2120.v1

physiology-first systems strategies may ultimately be able to cross boundary conditions from order to chaos or vice versa within subsets of the network.

Hence, the analysis and interpretation of redox proteomic datasets using information and chaos theory derived metrics can have important, far-reaching implications. In this light, redox proteomic data is no longer a snapshot—it is a time-warped map of system history, structure, and fate.

5. Conclusions

Erwin Schrodinger, Albert Szent-Györgyi and others are widely credited with the idea that discoveries consist of seeing what everybody else has seen and thinking what nobody else has thought. In this tradition, we have articulated a novel idea built atop what everybody in the field has seen—cysteine redox proteomic datasets.

We propose that these datasets can be reinterpreted through the lens of **information theory** and **chaos theory**—not just as static outputs but as **signals from dynamic systems,** revealing **geometry, structure, and unpredictability** in redox biology. From this perspective, a single oxidative shift could ripple over time crossing the chaotic boundary to a strange oxi-attractor—**the cysteine redox butterfly effect.**

Deriving novel insights does not depend on generating new data, but on rethinking what we already have. Petabytes of existing redox proteomic data can now be interrogated for **Shannon entropy, KL divergence, Fisher information, and chaos signatures**, extracting **hidden order and transitions** within complex peptide distribution**s. Hence, we expect these approaches to unlock latent patterns**, enabling not just new discoveries but a shift in how we **frame, model, and predict** dynamics in redox biology [231–233].

Information and chaos theory metrics can be applied to virtually every proteomic dataset from global label-free quantification [234] studies, targeted analyses [235–238], to advanced chemo-proteomic workflows [239], including reactive cysteine labelling [240–243] and PTMs like phosphorylation [244,245]. Other oxidative PTMs include methionine oxidation, tyrosine nitration, and carbonylation at several amino acids, such as lysine [246–257]. We fully expect similar insights to emerge from their reinterpretation. Hence, scientists across disparate fields can leverage information and chaos theory to derive novel proteomic insights from preexisting datasets [258].

In conclusion, we have reframed the analysis and interpretation of redox proteomic datasets, and potentially proteomic datasets at large, using mathematically grounded information and chaos theory derived metrics. The result is a new of thinking about redox biology—one that embraces the complexities and emergent properties of nonlinear dynamical systems.

Acknowledgments: The author thanks Prof. Angus Lamond (The University of Dundee) and the members of his lab for useful scientific discussions. During the preparation of this manuscript, the authors used *ChatGPT (OpenAI, GPT-4, July 2025)* for the purposes of idea refinement, language editing, figure caption ideas, symbolic visual inspiration, and high-level sound boarding. The tool was also used to provide structural feedback and enhance clarity during drafting. All content was reviewed, edited, and finalized by the authors, who take full responsibility for the accuracy and integrity of the publication.

Conflicts of Interest: The author declares no conflicts of interest.

References

1. Sies, H.; Mailloux, R.J.; Jakob, U. Fundamentals of Redox Regulation in Biology. *Nat. Rev. Mol. Cell Biol.* **2024**, 1–19, doi:10.1038/s41580-024-00730-2.
2. Alcock, L.J.; Perkins, M.V.; Chalker, J.M. Chemical Methods for Mapping Cysteine Oxidation. *Chem Soc Rev* **2017**, *47*, 231–268, doi:10.1039/c7cs00607a.
3. Paulsen, C.E.; Carroll, K.S. Cysteine-Mediated Redox Signaling: Chemistry, Biology, and Tools for Discovery. *Chem Rev* **2013**, *113*, 4633–4679, doi:10.1021/cr300163e.

 doi:10.20944/preprints202507.2120.v1

4. Gould, N.S.; Evans, P.; Martínez-Acedo, P.; Marino, S.M.; Gladyshev, V.N.; Carroll, K.S.; Ischiropoulos, H. Site-Specific Proteomic Mapping Identifies Selectively Modified Regulatory Cysteine Residues in Functionally Distinct Protein Networks. *Chem Biol* **2015**, *22*, 965–975, doi:10.1016/j.chembiol.2015.06.010.
5. Wensien, M.; Pappenheim, F.R. von; Funk, L.-M.; Kloskowski, P.; Curth, U.; Diederichsen, U.; Uranga, J.; Ye, J.; Fang, P.; Pan, K.-T.; et al. A Lysine–Cysteine Redox Switch with an NOS Bridge Regulates Enzyme Function. *Nature* **2021**, *593*, 460–464, doi:10.1038/s41586-021-03513-3.
6. Zhai, Y.; Chen, L.; Zhao, Q.; Zheng, Z.-H.; Chen, Z.-N.; Bian, H.; Yang, X.; Lu, H.-Y.; Lin, P.; Chen, X.; et al. Cysteine Carboxyethylation Generates Neoantigens to Induce HLA-Restricted Autoimmunity. *Science* **2023**, *379*, eabg2482, doi:10.1126/science.abg2482.
7. Huang, X.; Chen, S.; Li, W.; Tang, L.; Zhang, Y.; Yang, N.; Zou, Y.; Zhai, X.; Xiao, N.; Liu, W.; et al. ROS Regulated Reversible Protein Phase Separation Synchronizes Plant Flowering. *Nat Chem Biol* **2021**, *17*, 549–557, doi:10.1038/s41589-021-00739-0.
8. Lennicke, C.; Cochemé, H.M. Redox Metabolism: ROS as Specific Molecular Regulators of Cell Signaling and Function. *Mol Cell* **2021**, *81*, 3691–3707, doi:10.1016/j.molcel.2021.08.018.
9. Parvez, S.; Long, M.J.C.; Poganik, J.R.; Aye, Y. Redox Signaling by Reactive Electrophiles and Oxidants. *Chem Rev* **2018**, *118*, 8798–8888, doi:10.1021/acs.chemrev.7b00698.
10. Jones, D.P.; Sies, H. The Redox Code. *Antioxid Redox Sign* **2015**, *23*, 734–746, doi:10.1089/ars.2015.6247.
11. Jones, D.P. Redox Organization of Living Systems. *Free Radic. Biol. Med.* **2024**, *217*, 179–189, doi:10.1016/j.freeradbiomed.2024.03.008.
12. Feelisch, M.; Cortese-Krott, M.M.; Santolini, J.; Wootton, S.A.; Jackson, A.A. Systems Redox Biology in Health and Disease. *EXCLI J.* **2022**, *21*, 623–646, doi:10.17179/excli2022-4793.
13. Day, N.J.; Gaffrey, M.J.; Qian, W.-J. Stoichiometric Thiol Redox Proteomics for Quantifying Cellular Responses to Perturbations. *Antioxidants* **2021**, *10*, 499, doi:10.3390/antiox10030499.
14. Li, X.; Gluth, A.; Zhang, T.; Qian, W. Thiol Redox Proteomics: Characterization of Thiol-based Post-translational Modifications. *Proteomics* **2023**, e2200194, doi:10.1002/pmic.202200194.
15. Cobley, J.N.; Sakellariou, G.K.; Husi, H.; McDonagh, B. Proteomic Strategies to Unravel Age-Related Redox Signalling Defects in Skeletal Muscle. *Free Radical Bio Med* **2019**, *132*, 24–32, doi:10.1016/j.freeradbiomed.2018.09.012.
16. Kim, H.; Ha, S.; Lee, H.Y.; Lee, K. ROSics: Chemistry and Proteomics of Cysteine Modifications in Redox Biology. *Mass Spectrom Rev* **2015**, *34*, 184–208, doi:10.1002/mas.21430.
17. Burger, N.; Chouchani, E.T. A New Era of Cysteine Proteomics – Technological Advances in Thiol Biology. *Curr. Opin. Chem. Biol.* **2024**, *79*, 102435, doi:10.1016/j.cbpa.2024.102435.
18. Xiao, H.; Jedrychowski, M.P.; Schweppe, D.K.; Huttlin, E.L.; Yu, Q.; Heppner, D.E.; Li, J.; Long, J.; Mills, E.L.; Szpyt, J.; et al. A Quantitative Tissue-Specific Landscape of Protein Redox Regulation during Aging. *Cell* **2020**, *180*, 968-983.e24, doi:10.1016/j.cell.2020.02.012.
19. Li, X.; Day, N.J.; Feng, S.; Gaffrey, M.J.; Lin, T.-D.; Paurus, V.L.; Monroe, M.E.; Moore, R.J.; Yang, B.; Xian, M.; et al. Mass Spectrometry-Based Direct Detection of Multiple Types of Protein Thiol Modifications in Pancreatic Beta Cells under Endoplasmic Reticulum Stress. *Redox Biol* **2021**, *46*, 102111, doi:10.1016/j.redox.2021.102111.
20. Day, N.J.; Kelly, S.S.; Lui, L.; Mansfield, T.A.; Gaffrey, M.J.; Trejo, J.B.; Sagendorf, T.J.; Attah, I.K.; Moore, R.J.; Douglas, C.M.; et al. Signatures of Cysteine Oxidation on Muscle Structural and Contractile Proteins Are Associated with Physical Performance and Muscle Function in Older Adults: Study of Muscle, Mobility and Aging (SOMMA). *Aging Cell* **2024**, *23*, e14094, doi:10.1111/acel.14094.
21. Huang, J.; Staes, A.; Impens, F.; Demichev, V.; Breusegem, F.V.; Gevaert, K.; Willems, P. CysQuant: Simultaneous Quantification of Cysteine Oxidation and Protein Abundance Using Data Dependent or Independent Acquisition Mass Spectrometry. *Redox Biol.* **2023**, *67*, 102908, doi:10.1016/j.redox.2023.102908.
22. Anjo, S.I.; Melo, M.N.; Loureiro, L.R.; Sabala, L.; Castanheira, P.; Grãos, M.; Manadas, B. OxSWATH: An Integrative Method for a Comprehensive Redox-Centered Analysis Combined with a Generic Differential Proteomics Screening. *Redox Biol.* **2019**, *22*, 101130, doi:10.1016/j.redox.2019.101130.

 doi:10.20944/preprints202507.2120.v1

23. Behring, J.B.; Post, S. van der; Mooradian, A.D.; Egan, M.J.; Zimmerman, M.I.; Clements, J.L.; Bowman, G.R.; Held, J.M. Spatial and Temporal Alterations in Protein Structure by EGF Regulate Cryptic Cysteine Oxidation. *Sci Signal* **2020**, *13*, eaay7315, doi:10.1126/scisignal.aay7315.
24. Held, J.M. Redox Systems Biology: Harnessing the Sentinels of the Cysteine Redoxome. *Antioxid Redox Sign* **2020**, *32*, 659–676, doi:10.1089/ars.2019.7725.
25. Held, J.M.; Danielson, S.R.; Behring, J.B.; Atsriku, C.; Britton, D.J.; Puckett, R.L.; Schilling, B.; Campisi, J.; Benz, C.C.; Gibson, B.W. Targeted Quantitation of Site-Specific Cysteine Oxidation in Endogenous Proteins Using a Differential Alkylation and Multiple Reaction Monitoring Mass Spectrometry Approach. *Mol Cell Proteomics* **2010**, *9*, 1400–1410, doi:10.1074/mcp.m900643-mcp200.
26. Brown, G.C. Bioenergetic Myths of Energy Transduction in Eukaryotic Cells. *Front. Mol. Biosci.* **2024**, *11*, 1402910, doi:10.3389/fmolb.2024.1402910.
27. Cobley, J.N. 50 Shades of Oxidative Stress: A State-Specific Cysteine Redox Pattern Hypothesis. *Redox Biol.* **2023**, *67*, 102936, doi:10.1016/j.redox.2023.102936.
28. Lennicke, C.; Cochemé, H.M. Redox Regulation of the Insulin Signalling Pathway. *Redox Biol* **2021**, *42*, 101964, doi:10.1016/j.redox.2021.101964.
29. Sies, H. Oxidative Eustress: On Constant Alert for Redox Homeostasis. *Redox Biol* **2021**, *41*, 101867, doi:10.1016/j.redox.2021.101867.
30. Devant, P.; Boršić, E.; Ngwa, E.M.; Xiao, H.; Chouchani, E.T.; Thiagarajah, J.R.; Hafner-Bratkovič, I.; Evavold, C.L.; Kagan, J.C. Gasdermin D Pore-Forming Activity Is Redox-Sensitive. *Cell Reports* **2023**, *42*, 112008, doi:10.1016/j.celrep.2023.112008.
31. Cobley, J.N.; Fiorello, M.L.; Bailey, D.M. 13 Reasons Why the Brain Is Susceptible to Oxidative Stress. *Redox Biol* **2018**, *15*, 490–503, doi:10.1016/j.redox.2018.01.008.
32. Sies, H. Dynamics of Intracellular and Intercellular Redox Communication. *Free Radic. Biol. Med.* **2024**, *225*, 933–939, doi:10.1016/j.freeradbiomed.2024.11.002.
33. Shannon, C.E. A Mathematical Theory of Communication. *Bell Syst. Tech. J.* **1948**, *27*, 379–423, doi:10.1002/j.1538-7305.1948.tb01338.x.
34. D'Autréaux, B.; Toledano, M.B. ROS as Signalling Molecules: Mechanisms That Generate Specificity in ROS Homeostasis. *Nat Rev Mol Cell Bio* **2007**, *8*, 813–824, doi:10.1038/nrm2256.
35. Winterbourn, C.C.; Hampton, M.B. Thiol Chemistry and Specificity in Redox Signaling. *Free Radical Bio Med* **2008**, *45*, 549–561, doi:10.1016/j.freeradbiomed.2008.05.004.
36. Halliwell, B.; Gutteridge, J. *Free Radicals in Biology and Medicine*; 2015; Vol. 5th Edition;
37. Murphy, M.P.; Bayir, H.; Belousov, V.; Chang, C.J.; Davies, K.J.A.; Davies, M.J.; Dick, T.P.; Finkel, T.; Forman, H.J.; Janssen-Heininger, Y.; et al. Guidelines for Measuring Reactive Oxygen Species and Oxidative Damage in Cells and in Vivo. *Nat Metabolism* **2022**, *4*, 651–662, doi:10.1038/s42255-022-00591-z.
38. Halliwell, B. Understanding Mechanisms of Antioxidant Action in Health and Disease. *Nat. Rev. Mol. Cell Biol.* **2023**, 1–21, doi:10.1038/s41580-023-00645-4.
39. Murphy, M.P.; Holmgren, A.; Larsson, N.-G.; Halliwell, B.; Chang, C.J.; Kalyanaraman, B.; Rhee, S.G.; Thornalley, P.J.; Partridge, L.; Gems, D.; et al. Unraveling the Biological Roles of Reactive Oxygen Species. *Cell Metab* **2011**, *13*, 361–366, doi:10.1016/j.cmet.2011.03.010.
40. Sies, H.; Belousov, V.V.; Chandel, N.S.; Davies, M.J.; Jones, D.P.; Mann, G.E.; Murphy, M.P.; Yamamoto, M.; Winterbourn, C. Defining Roles of Specific Reactive Oxygen Species (ROS) in Cell Biology and Physiology. *Nat Rev Mol Cell Bio* **2022**, 1–17, doi:10.1038/s41580-022-00456-z.
41. Sies, H.; Jones, D.P. Reactive Oxygen Species (ROS) as Pleiotropic Physiological Signalling Agents. *Nat Rev Mol Cell Bio* **2020**, *21*, 363–383, doi:10.1038/s41580-020-0230-3.
42. Sies, H. Hydrogen Peroxide as a Central Redox Signaling Molecule in Physiological Oxidative Stress: Oxidative Eustress. *Redox Biol* **2017**, *11*, 613–619, doi:10.1016/j.redox.2016.12.035.
43. Moosmann, B.; Hajieva, P. Probing the Role of Cysteine Thiyl Radicals in Biology: Eminently Dangerous, Difficult to Scavenge. *Antioxidants* **2022**, *11*, 885, doi:10.3390/antiox11050885.
44. Margaritelis, N.V.; Cobley, J.N.; Paschalis, V.; Veskoukis, A.S.; Theodorou, A.A.; Kyparos, A.; Nikolaidis, M.G. Going Retro: Oxidative Stress Biomarkers in Modern Redox Biology. *Free Radical Bio Med* **2016**, *98*, 2–12, doi:10.1016/j.freeradbiomed.2016.02.005.

 doi:10.20944/preprints202507.2120.v1

45. Cobley, J.N.; Husi, H. Immunological Techniques to Assess Protein Thiol Redox State: Opportunities, Challenges and Solutions. *Antioxidants* **2020**, *9*, 315, doi:10.3390/antiox9040315.
46. Cobley, J.N. Mechanisms of Mitochondrial ROS Production in Assisted Reproduction: The Known, the Unknown, and the Intriguing. *Antioxidants* **2020**, *9*, 933, doi:10.3390/antiox9100933.
47. Margaritelis, N.V.; Cobley, J.N.; Paschalis, V.; Veskoukis, A.S.; Theodorou, A.A.; Kyparos, A.; Nikolaidis, M.G. Principles for Integrating Reactive Species into in Vivo Biological Processes: Examples from Exercise Physiology. *Cell Signal* **2016**, *28*, 256–271, doi:10.1016/j.cellsig.2015.12.011.
48. Cobley, J.N.; Margaritelis, N.V.; Chatzinikolaou, P.N.; Nikolaidis, M.G.; Davison, G.W. Ten "Cheat Codes" for Measuring Oxidative Stress in Humans. *Antioxidants* **2024**, *13*, 877, doi:10.3390/antiox13070877.
49. Choudhary, D.; Foster, K.R.; Uphoff, S. Chaos in a Bacterial Stress Response. *Curr. Biol.* **2023**, *33*, 5404-5414.e9, doi:10.1016/j.cub.2023.11.002.
50. Cobley, J.N. Oxiforms: Unique Cysteine Residue- and Chemotype-specified Chemical Combinations Can Produce Functionally-distinct Proteoforms. *Bioessays* **2023**, *45*, doi:10.1002/bies.202200248.
51. Desai, H.; Andrews, K.H.; Bergersen, K.V.; Ofori, S.; Yu, F.; Shikwana, F.; Arbing, M.A.; Boatner, L.M.; Villanueva, M.; Ung, N.; et al. Chemoproteogenomic Stratification of the Missense Variant Cysteinome. *Nat. Commun.* **2024**, *15*, 9284, doi:10.1038/s41467-024-53520-x.
52. Yan, T.; Boatner, L.M.; Cui, L.; Tontonoz, P.J.; Backus, K.M. Defining the Cell Surface Cysteinome Using Two-Step Enrichment Proteomics. *JACS Au* **2023**, *3*, 3506–3523, doi:10.1021/jacsau.3c00707.
53. Burton, N.R.; Polasky, D.A.; Shikwana, F.; Ofori, S.; Yan, T.; Geiszler, D.J.; Leprevost, F. da V.; Nesvizhskii, A.I.; Backus, K.M. Solid-Phase Compatible Silane-Based Cleavable Linker Enables Custom Isobaric Quantitative Chemoproteomics. *J. Am. Chem. Soc.* **2023**, *145*, 21303–21318, doi:10.1021/jacs.3c05797.
54. Desai, H.S.; Yan, T.; Yu, F.; Sun, A.W.; Villanueva, M.; Nesvizhskii, A.I.; Backus, K.M. SP3-Enabled Rapid and High Coverage Chemoproteomic Identification of Cell-State–Dependent Redox-Sensitive Cysteines. *Mol. Cell. Proteom.* **2022**, *21*, 100218, doi:10.1016/j.mcpro.2022.100218.
55. Yan, T.; Desai, H.S.; Boatner, L.M.; Yen, S.L.; Cao, J.; Palafox, M.F.; Jami-Alahmadi, Y.; Backus, K.M. SP3-FAIMS Chemoproteomics for High-Coverage Profiling of the Human Cysteinome**. *ChemBioChem* **2021**, *22*, 1841–1851, doi:10.1002/cbic.202000870.
56. Boatner, L.M.; Palafox, M.F.; Schweppe, D.K.; Backus, K.M. CysDB: A Human Cysteine Database Based on Experimental Quantitative Chemoproteomics. *Cell Chem Biol* **2023**, doi:10.1016/j.chembiol.2023.04.004.
57. Yan, T.; Palmer, A.B.; Geiszler, D.J.; Polasky, D.A.; Boatner, L.M.; Burton, N.R.; Armenta, E.; Nesvizhskii, A.I.; Backus, K.M. Enhancing Cysteine Chemoproteomic Coverage through Systematic Assessment of Click Chemistry Product Fragmentation. *Anal Chem* **2022**, *94*, 3800–3810, doi:10.1021/acs.analchem.1c04402.
58. Huang, H.; Petersen, M.H.; Ibañez-Vea, M.; Lassen, P.S.; Larsen, M.R.; Palmisano, G. Simultaneous Enrichment of Cysteine-Containing Peptides and Phosphopeptides Using a Cysteine-Specific Phosphonate Adaptable Tag (CysPAT) in Combination with Titanium Dioxide (TiO2) Chromatography*. *Mol. Cell. Proteom.* **2016**, *15*, 3282–3296, doi:10.1074/mcp.m115.054551.
59. Leichert, L.I.; Gehrke, F.; Gudiseva, H.V.; Blackwell, T.; Ilbert, M.; Walker, A.K.; Strahler, J.R.; Andrews, P.C.; Jakob, U. Quantifying Changes in the Thiol Redox Proteome upon Oxidative Stress in Vivo. *Proc National Acad Sci* **2008**, *105*, 8197–8202, doi:10.1073/pnas.0707723105.
60. Chouchani, E.T.; Methner, C.; Nadtochiy, S.M.; Logan, A.; Pell, V.R.; Ding, S.; James, A.M.; Cochemé, H.M.; Reinhold, J.; Lilley, K.S.; et al. Cardioprotection by S-Nitrosation of a Cysteine Switch on Mitochondrial Complex I. *Nat Med* **2013**, *19*, 753–759, doi:10.1038/nm.3212.
61. Chouchani, E.T.; James, A.M.; Fearnley, I.M.; Lilley, K.S.; Murphy, M.P. Proteomic Approaches to the Characterization of Protein Thiol Modification. *Curr Opin Chem Biol* **2011**, *15*, 120–128, doi:10.1016/j.cbpa.2010.11.003.
62. Sinha, A.; Mann, M. A Beginner's Guide to Mass Spectrometry–Based Proteomics. *Biochem.* **2020**, *42*, 64–69, doi:10.1042/bio20200057.
63. Aebersold, R.; Mann, M. Mass Spectrometry-Based Proteomics. *Nature* **2003**, *422*, 198–207, doi:10.1038/nature01511.
64. Steen, H.; Mann, M. The Abc's (and Xyz's) of Peptide Sequencing. *Nat Rev Mol Cell Bio* **2004**, *5*, 699–711, doi:10.1038/nrm1468.

 doi:10.20944/preprints202507.2120.v1

65. He, F.; Aebersold, R.; Baker, M.S.; Bian, X.; Bo, X.; Chan, D.W.; Chang, C.; Chen, L.; Chen, X.; Chen, Y.-J.; et al. π-HuB: The Proteomic Navigator of the Human Body. *Nature* **2024**, *636*, 322–331, doi:10.1038/s41586-024-08280-5.
66. Guo, T.; Steen, J.A.; Mann, M. Mass-Spectrometry-Based Proteomics: From Single Cells to Clinical Applications. *Nature* **2025**, *638*, 901–911, doi:10.1038/s41586-025-08584-0.
67. Aebersold, R.; Mann, M. Mass-Spectrometric Exploration of Proteome Structure and Function. *Nature* **2016**, *537*, 347–355, doi:10.1038/nature19949.
68. Cox, J.; Mann, M. MaxQuant Enables High Peptide Identification Rates, Individualized p.p.b.-Range Mass Accuracies and Proteome-Wide Protein Quantification. *Nat. Biotechnol.* **2008**, *26*, 1367–1372, doi:10.1038/nbt.1511.
69. Demichev, V.; Messner, C.B.; Vernardis, S.I.; Lilley, K.S.; Ralser, M. DIA-NN: Neural Networks and Interference Correction Enable Deep Proteome Coverage in High Throughput. *Nat. Methods* **2020**, *17*, 41–44, doi:10.1038/s41592-019-0638-x.
70. Lou, R.; Cao, Y.; Li, S.; Lang, X.; Li, Y.; Zhang, Y.; Shui, W. Benchmarking Commonly Used Software Suites and Analysis Workflows for DIA Proteomics and Phosphoproteomics. *Nat. Commun.* **2023**, *14*, 94, doi:10.1038/s41467-022-35740-1.
71. Pillay, C.S.; Eagling, B.D.; Driscoll, S.R.E.; Rohwer, J.M. Quantitative Measures for Redox Signaling. *Free Radical Bio Med* **2016**, *96*, 290–303, doi:10.1016/j.freeradbiomed.2016.04.199.
72. Buettner, G.R.; Wagner, B.A.; Rodgers, V.G.J. Quantitative Redox Biology: An Approach to Understand the Role of Reactive Species in Defining the Cellular Redox Environment. *Cell Biochem Biophys* **2013**, *67*, 477–483, doi:10.1007/s12013-011-9320-3.
73. Cobley, J.N.; Moult, P.R.; Burniston, J.G.; Morton, J.P.; Close, G.L. Exercise Improves Mitochondrial and Redox-Regulated Stress Responses in the Elderly: Better Late than Never! *Biogerontology* **2015**, *16*, 249–264, doi:10.1007/s10522-014-9546-8.
74. Cobley, J.N.; Sakellariou, G.K.; Owens, D.J.; Murray, S.; Waldron, S.; Gregson, W.; Fraser, W.D.; Burniston, J.G.; Iwanejko, L.A.; McArdle, A.; et al. Lifelong Training Preserves Some Redox-Regulated Adaptive Responses after an Acute Exercise Stimulus in Aged Human Skeletal Muscle. *Free Radical Bio Med* **2014**, *70*, 23–32, doi:10.1016/j.freeradbiomed.2014.02.004.
75. Stretton, C.; Pugh, J.N.; McDonagh, B.; McArdle, A.; Close, G.L.; Jackson, M.J. 2-Cys Peroxiredoxin Oxidation in Response to Hydrogen Peroxide and Contractile Activity in Skeletal Muscle: A Novel Insight into Exercise-Induced Redox Signalling? *Free Radical Bio Med* **2020**, *160*, 199–207, doi:10.1016/j.freeradbiomed.2020.06.020.
76. Pugh, J.N.; Stretton, C.; McDonagh, B.; Brownridge, P.; McArdle, A.; Jackson, M.J.; Close, G.L. Exercise Stress Leads to an Acute Loss of Mitochondrial Proteins and Disruption of Redox Control in Skeletal Muscle of Older Subjects: An Underlying Decrease in Resilience with Aging? *Free Radical Bio Med* **2021**, *177*, 88–99, doi:10.1016/j.freeradbiomed.2021.10.003.
77. McDonagh, B.; Sakellariou, G.K.; Smith, N.T.; Brownridge, P.; Jackson, M.J. Differential Cysteine Labeling and Global Label-Free Proteomics Reveals an Altered Metabolic State in Skeletal Muscle Aging. *J. Proteome Res.* **2014**, *13*, 5008–5021, doi:10.1021/pr5006394.
78. Shinn, M. Phantom Oscillations in Principal Component Analysis. *Proc. Natl. Acad. Sci.* **2023**, *120*, e2311420120, doi:10.1073/pnas.2311420120.
79. Urrutia, P.J.; Bórquez, D.A. Expanded Bioinformatic Analysis of Oximouse Dataset Reveals Key Putative Processes Involved in Brain Aging and Cognitive Decline. *Free Radic. Biol. Med.* **2023**, *207*, 200–211, doi:10.1016/j.freeradbiomed.2023.07.018.
80. Kitano, H. Computational Systems Biology. *Nature* **2002**, *420*, 206–210, doi:10.1038/nature01254.
81. Hartwell, L.H.; Hopfield, J.J.; Leibler, S.; Murray, A.W. From Molecular to Modular Cell Biology. *Nature* **1999**, *402*, C47–C52, doi:10.1038/35011540.
82. Smith, L.M.; Kelleher, N.L.; Linial, M.; Goodlett, D.; Langridge-Smith, P.; Goo, Y.A.; Safford, G.; Bonilla*, L.; Kruppa, G.; Zubarev, R.; et al. Proteoform: A Single Term Describing Protein Complexity. *Nat Methods* **2013**, *10*, 186–187, doi:10.1038/nmeth.2369.

 doi:10.20944/preprints202507.2120.v1

83. Smith, L.M.; Kelleher, N.L. Proteoforms as the next Proteomics Currency. *Science* **2018**, *359*, 1106–1107, doi:10.1126/science.aat1884.
84. Carbonara, K.; Andonovski, M.; Coorssen, J.R. Proteomes Are of Proteoforms: Embracing the Complexity. *Proteomes* **2021**, *9*, 38, doi:10.3390/proteomes9030038.
85. Coorssen, J.R.; Padula, M.P. Proteomics—The State of the Field: The Definition and Analysis of Proteomes Should Be Based in Reality, Not Convenience. *Proteomes* **2024**, *12*, 14, doi:10.3390/proteomes12020014.
86. Alfaro, J.A.; Bohländer, P.; Dai, M.; Filius, M.; Howard, C.J.; Kooten, X.F. van; Ohayon, S.; Pomorski, A.; Schmid, S.; Aksimentiev, A.; et al. The Emerging Landscape of Single-Molecule Protein Sequencing Technologies. *Nat Methods* **2021**, *18*, 604–617, doi:10.1038/s41592-021-01143-1.
87. Cobley, J.N. Exploring the Unmapped Cysteine Redox Proteoform Landscape. *Am. J. Physiol.-Cell Physiol.* **2024**, doi:10.1152/ajpcell.00152.2024.
88. Parkies, S.L.; Lind, D.J.; Pillay, C.S. Emerging Trends for the Regulation of Thiol-Based Redox Transcription Factor Pathways. *Biochemistry* **2025**, doi:10.1021/acs.biochem.5c00268.
89. Jacquel, B.; Kavčič, B.; Aspert, T.; Matifas, A.; Kuehn, A.; Zhuravlev, A.; Byckov, E.; Morgan, B.; Julou, T.; Charvin, G. A Trade-off between Stress Resistance and Tolerance Underlies the Adaptive Response to Hydrogen Peroxide. *Cell Syst.* **2025**, 101320, doi:10.1016/j.cels.2025.101320.
90. Lind, D.J.; Naidoo, K.C.; Tomalin, L.E.; Rohwer, J.M.; Veal, E.A.; Pillay, C.S. Quantifying Redox Transcription Factor Dynamics as a Tool to Investigate Redox Signalling. *Free Radic. Biol. Med.* **2024**, *218*, 16–25, doi:10.1016/j.freeradbiomed.2024.04.004.
91. Smith, L.M.; Thomas, P.M.; Shortreed, M.R.; Schaffer, L.V.; Fellers, R.T.; LeDuc, R.D.; Tucholski, T.; Ge, Y.; Agar, J.N.; Anderson, L.C.; et al. A Five-Level Classification System for Proteoform Identifications. *Nat. Methods* **2019**, *16*, 939–940, doi:10.1038/s41592-019-0573-x.
92. Bamberger, C.; Martínez-Bartolomé, S.; Montgomery, M.; Pankow, S.; Hulleman, J.D.; Kelly, J.W.; Yates, J.R. Deducing the Presence of Proteins and Proteoforms in Quantitative Proteomics. *Nat. Commun.* **2018**, *9*, 2320, doi:10.1038/s41467-018-04411-5.
93. Aebersold, R.; Agar, J.N.; Amster, I.J.; Baker, M.S.; Bertozzi, C.R.; Boja, E.S.; Costello, C.E.; Cravatt, B.F.; Fenselau, C.; Garcia, B.A.; et al. How Many Human Proteoforms Are There? *Nat Chem Biol* **2018**, *14*, 206–214, doi:10.1038/nchembio.2576.
94. Marx, V. Inside the Chase after Those Elusive Proteoforms. *Nat. Methods* **2024**, 1–6, doi:10.1038/s41592-024-02170-4.
95. Bludau, I.; Aebersold, R. Proteomic and Interactomic Insights into the Molecular Basis of Cell Functional Diversity. *Nat. Rev. Mol. Cell Biol.* **2020**, *21*, 327–340, doi:10.1038/s41580-020-0231-2.
96. Cobley, J.N.; Chatzinikolaou, P.N.; Schmidt, C.A. Computational Analysis of Human Cysteine Redox Proteoforms Reveals Novel Insights., doi:10.1101/2024.09.18.613618.
97. Cobley, J.N.; Chatzinikolaou, P.N.; Schmidt, C.A. The Nonlinear Cysteine Redox Dynamics in the I-Space: A Proteoform-Centric Theory of Redox Regulation. *Redox Biol.* **2025**, 103523, doi:10.1016/j.redox.2025.103523.
98. Hansen, R.E.; Roth, D.; Winther, J.R. Quantifying the Global Cellular Thiol–Disulfide Status. *Proc National Acad Sci* **2009**, *106*, 422–427, doi:10.1073/pnas.0812149106.
99. Cobley, J.N.; Noble, A.; Guille, M. Cleland Immunoblotting Unmasks Unexpected Cysteine Redox Proteoforms., doi:10.1101/2024.09.18.613741.
100. Melani, R.D.; Gerbasi, V.R.; Anderson, L.C.; Sikora, J.W.; Toby, T.K.; Hutton, J.E.; Butcher, D.S.; Negrão, F.; Seckler, H.S.; Srzentić, K.; et al. The Blood Proteoform Atlas: A Reference Map of Proteoforms in Human Hematopoietic Cells. *Science* **2022**, *375*, 411–418, doi:10.1126/science.aaz5284.
101. Smith, L.M.; Agar, J.N.; Chamot-Rooke, J.; Danis, P.O.; Ge, Y.; Loo, J.A.; Paša-Tolić, L.; Tsybin, Y.O.; Kelleher, N.L.; Proteomics, T.C. for T.-D. The Human Proteoform Project: Defining the Human Proteome. *Sci Adv* **2021**, *7*, eabk0734, doi:10.1126/sciadv.abk0734.
102. Roberts, D.S.; Loo, J.A.; Tsybin, Y.O.; Liu, X.; Wu, S.; Chamot-Rooke, J.; Agar, J.N.; Paša-Tolić, L.; Smith, L.M.; Ge, Y. Top-down Proteomics. *Nat. Rev. Methods Prim.* **2024**, *4*, 38, doi:10.1038/s43586-024-00318-2.

 doi:10.20944/preprints202507.2120.v1

103. Burnum-Johnson, K.E.; Conrads, T.P.; Drake, R.R.; Herr, A.E.; Iyengar, R.; Kelly, R.T.; Lundberg, E.; MacCoss, M.J.; Naba, A.; Nolan, G.P.; et al. New Views of Old Proteins: Clarifying the Enigmatic Proteome. *Mol Cell Proteomics* **2022**, *21*, 100254, doi:10.1016/j.mcpro.2022.100254.
104. Su, P.; Hollas, M.A.R.; Pla, I.; Rubakhin, S.; Butun, F.A.; Greer, J.B.; Early, B.P.; Fellers, R.T.; Caldwell, M.A.; Sweedler, J.V.; et al. Proteoform Profiling of Endogenous Single Cells from Rat Hippocampus at Scale. *Nat. Biotechnol.* **2025**, 1–5, doi:10.1038/s41587-025-02669-x.
105. Plubell, D.L.; Käll, L.; Webb-Robertson, B.-J.; Bramer, L.M.; Ives, A.; Kelleher, N.L.; Smith, L.M.; Montine, T.J.; Wu, C.C.; MacCoss, M.J. Putting Humpty Dumpty Back Together Again: What Does Protein Quantification Mean in Bottom-Up Proteomics? *J. Proteome Res.* **2022**, *21*, 891–898, doi:10.1021/acs.jproteome.1c00894.
106. Pace, P.E.; Fu, L.; Hampton, M.B.; Winterbourn, C.C. Redox Proteomic Analysis of H2O2 -Treated Jurkat Cells and Effects of Bicarbonate and Knockout of Peroxiredoxins 1 and 2. *Free Radic. Biol. Med.* **2025**, *227*, 221–232, doi:10.1016/j.freeradbiomed.2024.10.314.
107. Ivancevic, V.G.; Ivancevic, T.T. Ricci Flow and Nonlinear Reaction–Diffusion Systems in Biology, Chemistry, and Physics. *Nonlinear Dyn.* **2011**, *65*, 35–54, doi:10.1007/s11071-010-9872-6.
108. Heppner, D.E.; Dustin, C.M.; Liao, C.; Hristova, M.; Veith, C.; Little, A.C.; Ahlers, B.A.; White, S.L.; Deng, B.; Lam, Y.-W.; et al. Direct Cysteine Sulfenylation Drives Activation of the Src Kinase. *Nat Commun* **2018**, *9*, 4522, doi:10.1038/s41467-018-06790-1.
109. Wani, R.; Qian, J.; Yin, L.; Bechtold, E.; King, S.B.; Poole, L.B.; Paek, E.; Tsang, A.W.; Furdui, C.M. Isoform-Specific Regulation of Akt by PDGF-Induced Reactive Oxygen Species. *Proc National Acad Sci* **2011**, *108*, 10550–10555, doi:10.1073/pnas.1011665108.
110. Su, Z.; Burchfield, J.G.; Yang, P.; Humphrey, S.J.; Yang, G.; Francis, D.; Yasmin, S.; Shin, S.-Y.; Norris, D.M.; Kearney, A.L.; et al. Global Redox Proteome and Phosphoproteome Analysis Reveals Redox Switch in Akt. *Nat Commun* **2019**, *10*, 5486, doi:10.1038/s41467-019-13114-4.
111. Zhang, J.; Ali, M.Y.; Chong, H.B.; Tien, P.-C.; Woods, J.; Noble, C.; Vornbäumen, T.; Ordulu, Z.; Possemato, A.P.; Harry, S.; et al. Oxidation of Retromer Complex Controls Mitochondrial Translation. *Nature* **2025**, 1–11, doi:10.1038/s41586-025-08756-y.
112. Huang, J.; Co, H.K.; Lee, Y.; Wu, C.; Chen, S. Multistability Maintains Redox Homeostasis in Human Cells. *Mol. Syst. Biol.* **2021**, *17*, e10480, doi:10.15252/msb.202110480.
113. Feinstein, A. A New Basic Theorem of Information Theory. *Trans. IRE Prof. Group Inf. Theory* **1954**, *4*, 2–22, doi:10.1109/tit.1954.1057459.
114. Nunn, A.V.W.; Guy, G.W.; Bell, J.D. The Quantum Mitochondrion and Optimal Health. *Biochem. Soc. Trans.* **2016**, *44*, 1101–1110, doi:10.1042/bst20160096.
115. Waltermann, C.; Klipp, E. Information Theory Based Approaches to Cellular Signaling. *Biochim. Biophys. Acta (BBA) - Gen. Subj.* **2011**, *1810*, 924–932, doi:10.1016/j.bbagen.2011.07.009.
116. Lu, Y.R.; Tian, X.; Sinclair, D.A. The Information Theory of Aging. *Nat. Aging* **2023**, *3*, 1486–1499, doi:10.1038/s43587-023-00527-6.
117. Malakoff, D. Bayes Offers a "New" Way to Make Sense of Numbers. *Science* **1999**, *286*, 1460–1464, doi:10.1126/science.286.5444.1460.
118. Crutchfield, J.P.; Young, K. Inferring Statistical Complexity. *Phys. Rev. Lett.* **1989**, *63*, 105–108, doi:10.1103/physrevlett.63.105.
119. Lorenz, E.N. Deterministic Nonperiodic Flow. *J. Atmos. Sci.* **1963**, *20*, 130–141, doi:10.1175/1520-0469(1963)020<0130:dnf>2.0.co;2.
120. Gleick, J. *Chaos: Making the New Science*; Penguin Books, 2008; ISBN 9780143113454.
121. Lorenz, E.N. Predictability: Does the Flap of a Butterfly's Wings in Brazil Set off a Tornado in Texas. In Proceedings of the merican Association for the Advancement of Science; Washington DC, 1972.
122. Feigenbaum, M.J. Quantitative Universality for a Class of Nonlinear Transformations. *J. Stat. Phys.* **1978**, *19*, 25–52, doi:10.1007/bf01020332.
123. Mandelbrot, B.B. Fractals in Physics: Squig Clusters, Diffusions, Fractal Measures, and the Unicity of Fractal Dimensionality. *J. Stat. Phys.* **1984**, *34*, 895–930, doi:10.1007/bf01009448.

 doi:10.20944/preprints202507.2120.v1

124. Mandelbrot, B.B. Fractal Geometry: What Is It, and What Does It Do? *Proc. R. Soc. Lond. A Math. Phys. Sci.* **1989**, *423*, 3–16, doi:10.1098/rspa.1989.0038.
125. Gutteridge, J.M.C.; Halliwell, B. Mini-Review: Oxidative Stress, Redox Stress or Redox Success? *Biochem Bioph Res Co* **2018**, *502*, 183–186, doi:10.1016/j.bbrc.2018.05.045.
126. Halliwell, B. Biochemistry of Oxidative Stress. *Biochemical Society Transactions* **2007**.
127. Paulsen, C.E.; Truong, T.H.; Garcia, F.J.; Homann, A.; Gupta, V.; Leonard, S.E.; Carroll, K.S. Peroxide-Dependent Sulfenylation of the EGFR Catalytic Site Enhances Kinase Activity. *Nat Chem Biol* **2012**, *8*, 57–64, doi:10.1038/nchembio.736.
128. Go, Y.-M.; Chandler, J.D.; Jones, D.P. The Cysteine Proteome. *Free Radical Bio Med* **2015**, *84*, 227–245, doi:10.1016/j.freeradbiomed.2015.03.022.
129. Go, Y.-M.; Roede, J.R.; Walker, D.I.; Duong, D.M.; Seyfried, N.T.; Orr, M.; Liang, Y.; Pennell, K.D.; Jones, D.P. Selective Targeting of the Cysteine Proteome by Thioredoxin and Glutathione Redox Systems*. *Mol Cell Proteomics* **2013**, *12*, 3285–3296, doi:10.1074/mcp.m113.030437.
130. Moan, N.L.; Clement, G.; Maout, S.L.; Tacnet, F.; Toledano, M.B. The Saccharomyces Cerevisiae Proteome of Oxidized Protein Thiols CONTRASTED FUNCTIONS FOR THE THIOREDOXIN AND GLUTATHIONE PATHWAYS*. *J Biol Chem* **2006**, *281*, 10420–10430, doi:10.1074/jbc.m513346200.
131. Reest, J. van der; Lilla, S.; Zheng, L.; Zanivan, S.; Gottlieb, E. Proteome-Wide Analysis of Cysteine Oxidation Reveals Metabolic Sensitivity to Redox Stress. *Nat Commun* **2018**, *9*, 1581, doi:10.1038/s41467-018-04003-3.
132. Cobley, J.N.; Close, G.L.; Bailey, D.M.; Davison, G.W. Exercise Redox Biochemistry: Conceptual, Methodological and Technical Recommendations. *Redox Biol* **2017**, *12*, 540–548, doi:10.1016/j.redox.2017.03.022.
133. Cobley, J.N. Oxidative Stress. **2020**, 447–462, doi:10.1016/b978-0-12-818606-0.00023-7.
134. Cobley, J.N.; Davison, G.W. Oxidative Eustress in Exercise Physiology. **2022**, 11–22, doi:10.1201/9781003051619-2.
135. Cobley, James.N.; Davison, G.W. *Oxidative Eustress in Exercise Physiology*; CRC Press, 2022; ISBN 9781003051619.
136. Cobley, J.N.; Margaritelis, N.V.; Morton, J.P.; Close, G.L.; Nikolaidis, M.G.; Malone, J.K. The Basic Chemistry of Exercise-Induced DNA Oxidation: Oxidative Damage, Redox Signaling, and Their Interplay. *Front Physiol* **2015**, *6*, 182, doi:10.3389/fphys.2015.00182.
137. Nikolaidis, M.G.; Margaritelis, N.V. Free Radicals and Antioxidants: Appealing to Magic. *Trends Endocrinol. Metab.* **2023**, doi:10.1016/j.tem.2023.06.001.
138. Nikolaidis, M.; Margaritelis, N.; Matsakas, A. Quantitative Redox Biology of Exercise. *Int. J. Sports Med.* **2020**, *41*, 633–645, doi:10.1055/a-1157-9043.
139. Margaritelis, N.V.; Chatzinikolaou, P.N.; Chatzinikolaou, A.N.; Paschalis, V.; Theodorou, A.A.; Vrabas, I.S.; Kyparos, A.; Nikolaidis, M.G. The Redox Signal: A Physiological Perspective. *IUBMB Life* **2022**, *74*, 29–40, doi:10.1002/iub.2550.
140. Margaritelis, N.V.; Cobley, J.N.; Nastos, G.G.; Papanikolaou, K.; Bailey, S.J.; Kritsiligkou, P.; Nikolaidis, M.G. "Unlocking Athletic Potential: Exploring Exercise Physiology from Mechanisms to Performance": Evidence-Based Sports Supplements: A Redox Analysis. *Free Radic. Biol. Med.* **2024**, *224*, 62–77, doi:10.1016/j.freeradbiomed.2024.08.012.
141. Ursini, F.; Maiorino, M.; Forman, H.J. Redox Homeostasis: The Golden Mean of Healthy Living. *Redox Biol* **2016**, *8*, 205–215, doi:10.1016/j.redox.2016.01.010.
142. Marinho, H.S.; Real, C.; Cyrne, L.; Soares, H.; Antunes, F. Hydrogen Peroxide Sensing, Signaling and Regulation of Transcription Factors. *Redox Biol* **2014**, *2*, 535–562, doi:10.1016/j.redox.2014.02.006.
143. Antunes, F.; Brito, P.M. Quantitative Biology of Hydrogen Peroxide Signaling. *Redox Biol* **2017**, *13*, 1–7, doi:10.1016/j.redox.2017.04.039.
144. Meng, J.; Lv, Z.; Wang, Y.; Chen, C. Identification of the Redox-Stress Signaling Threshold (RST): Increased RST Helps to Delay Aging in C. Elegans. *Free Radical Bio Med* **2021**, *178*, 54–58, doi:10.1016/j.freeradbiomed.2021.11.018.
145. Sies, H.; Berndt, C.; Jones, D.P. Oxidative Stress. *Annu Rev Biochem* **2016**, *86*, 1–34, doi:10.1146/annurev-biochem-061516-045037.

 doi:10.20944/preprints202507.2120.v1

146. Sies, H. Oxidative Stress: A Concept in Redox Biology and Medicine. *Redox Biol* **2015**, *4*, 180–183, doi:10.1016/j.redox.2015.01.002.
147. Sies, H. Oxidative Stress: Concept and Some Practical Aspects. *Antioxidants* **2020**, *9*, 852, doi:10.3390/antiox9090852.
148. Lloyd, D.; Aon, M.A.; Cortassa, S. Why Homeodynamics, Not Homeostasis? *Sci. World J.* **2001**, *1*, 133–145, doi:10.1100/tsw.2001.20.
149. Forman, H.J.; Zhang, H. Targeting Oxidative Stress in Disease: Promise and Limitations of Antioxidant Therapy. *Nat Rev Drug Discov* **2021**, 1–21, doi:10.1038/s41573-021-00233-1.
150. Robb, E.L.; Gawel, J.M.; Aksentijević, D.; Cochemé, H.M.; Stewart, T.S.; Shchepinova, M.M.; Qiang, H.; Prime, T.A.; Bright, T.P.; James, A.M.; et al. Selective Superoxide Generation within Mitochondria by the Targeted Redox Cycler MitoParaquat. *Free Radical Bio Med* **2015**, *89*, 883–894, doi:10.1016/j.freeradbiomed.2015.08.021.
151. Booty, L.M.; Gawel, J.M.; Cvetko, F.; Caldwell, S.T.; Hall, A.R.; Mulvey, J.F.; James, A.M.; Hinchy, E.C.; Prime, T.A.; Arndt, S.; et al. Selective Disruption of Mitochondrial Thiol Redox State in Cells and In Vivo. *Cell Chem Biol* **2019**, *26*, 449-461.e8, doi:10.1016/j.chembiol.2018.12.002.
152. Sidlauskaite, E.; Gibson, J.W.; Megson, I.L.; Whitfield, P.D.; Tovmasyan, A.; Batinic-Haberle, I.; Murphy, M.P.; Moult, P.R.; Cobley, J.N. Mitochondrial ROS Cause Motor Deficits Induced by Synaptic Inactivity: Implications for Synapse Pruning. *Redox Biol* **2018**, *16*, 344–351, doi:10.1016/j.redox.2018.03.012.
153. Murphy, M.P. How Mitochondria Produce Reactive Oxygen Species. *Biochem J* **2009**, *417*, 1–13, doi:10.1042/bj20081386.
154. Cho, C.-S.; Yoon, H.J.; Kim, J.Y.; Woo, H.A.; Rhee, S.G. Circadian Rhythm of Hyperoxidized Peroxiredoxin II Is Determined by Hemoglobin Autoxidation and the 20S Proteasome in Red Blood Cells. *Proc National Acad Sci* **2014**, *111*, 12043–12048, doi:10.1073/pnas.1401100111.
155. O'Neill, J.S.; Ooijen, G. van; Dixon, L.E.; Troein, C.; Corellou, F.; Bouget, F.-Y.; Reddy, A.B.; Millar, A.J. Circadian Rhythms Persist without Transcription in a Eukaryote. *Nature* **2011**, *469*, 554–558, doi:10.1038/nature09654.
156. Pei, J.-F.; Li, X.-K.; Li, W.-Q.; Gao, Q.; Zhang, Y.; Wang, X.-M.; Fu, J.-Q.; Cui, S.-S.; Qu, J.-H.; Zhao, X.; et al. Diurnal Oscillations of Endogenous H2O2 Sustained by P66Shc Regulate Circadian Clocks. *Nat Cell Biol* **2019**, *21*, 1553–1564, doi:10.1038/s41556-019-0420-4.
157. Amponsah, P.S.; Yahya, G.; Zimmermann, J.; Mai, M.; Mergel, S.; Mühlhaus, T.; Storchova, Z.; Morgan, B. Peroxiredoxins Couple Metabolism and Cell Division in an Ultradian Cycle. *Nat Chem Biol* **2021**, *17*, 477–484, doi:10.1038/s41589-020-00728-9.
158. Bazopoulou, D.; Knoefler, D.; Zheng, Y.; Ulrich, K.; Oleson, B.J.; Xie, L.; Kim, M.; Kaufmann, A.; Lee, Y.-T.; Dou, Y.; et al. Developmental ROS Individualizes Organismal Stress Resistance and Lifespan. *Nature* **2019**, *576*, 301–305, doi:10.1038/s41586-019-1814-y.
159. Cobley, J.N. Synapse Pruning: Mitochondrial ROS with Their Hands on the Shears. *Bioessays* **2018**, *40*, 1800031, doi:10.1002/bies.201800031.
160. Foyer, C.H.; Wilson, M.H.; Wright, M.H. Redox Regulation of Cell Proliferation: Bioinformatics and Redox Proteomics Approaches to Identify Redox-Sensitive Cell Cycle Regulators. *Free Radical Bio Med* **2018**, *122*, 137–149, doi:10.1016/j.freeradbiomed.2018.03.047.
161. Henau, S.D.; Pagès-Gallego, M.; Pannekoek, W.-J.; Dansen, T.B. Mitochondria-Derived H2O2 Promotes Symmetry Breaking of the C. Elegans Zygote. *Dev Cell* **2020**, *53*, 263-271.e6, doi:10.1016/j.devcel.2020.03.008.
162. Cobley, J.; Noble, A.; Bessell, R.; Guille, M.; Husi, H. Reversible Thiol Oxidation Inhibits the Mitochondrial ATP Synthase in Xenopus Laevis Oocytes. *Antioxidants* **2020**, *9*, 215, doi:10.3390/antiox9030215.
163. LYAPUNOV, A.M. The General Problem of the Stability of Motion. *Int. J. Control* **1992**, *55*, 531–534, doi:10.1080/00207179208934253.
164. Wolf, A.; Swift, J.B.; Swinney, H.L.; Vastano, J.A. Determining Lyapunov Exponents from a Time Series. *Phys. D: Nonlinear Phenom.* **1985**, *16*, 285–317, doi:10.1016/0167-2789(85)90011-9.
165. Eckmann, J.-P.; Ruelle, D. Ergodic Theory of Chaos and Strange Attractors. *Rev. Mod. Phys.* **1985**, *57*, 617–656, doi:10.1103/revmodphys.57.617.

 doi:10.20944/preprints202507.2120.v1

166. Pincus, S.M. Approximate Entropy as a Measure of System Complexity. *Proc. Natl. Acad. Sci.* **1991**, *88*, 2297–2301, doi:10.1073/pnas.88.6.2297.
167. Grassberger, P.; Procaccia, I. Characterization of Strange Attractors. *Phys. Rev. Lett.* **1982**, *50*, 346–349, doi:10.1103/physrevlett.50.346.
168. Marwan, N.; Romano, M.C.; Thiel, M.; Kurths, J. Recurrence Plots for the Analysis of Complex Systems. *Phys. Rep.* **2007**, *438*, 237–329, doi:10.1016/j.physrep.2006.11.001.
169. Kirova, D.G.; Judasova, K.; Vorhauser, J.; Zerjatke, T.; Leung, J.K.; Glauche, I.; Mansfeld, J. A ROS-Dependent Mechanism Promotes CDK2 Phosphorylation to Drive Progression through S Phase. *Dev Cell* **2022**, *57*, 1712–1727, doi:10.1016/j.devcel.2022.06.008.
170. Vorhauser, J.; Roumeliotis, T.I.; Leung, J.K.; Coupe, D.; Yu, L.; Böhlig, K.; Nadler, A.; Choudhary, J.S.; Mansfeld, J. Cell Cycle-Dependent S-Sulfenyl Proteomics Uncover a Redox Switch in P21-CDK Feedback Governing the Proliferation-Senescence Decision. *bioRxiv* **2024**, 2024.09.14.613007, doi:10.1101/2024.09.14.613007.
171. Henríquez-Olguín, C.; Gallero, S.; Reddy, A.; Persson, K.W.; Schlabs, F.L.; Voldstedlund, C.T.; Valentinaviciute, G.; Meneses-Valdés, R.; Sigvardsen, C.M.; Kiens, B.; et al. Revisiting Insulin-Stimulated Hydrogen Peroxide Dynamics Reveals a Cytosolic Reductive Shift in Skeletal Muscle. *Redox Biol.* **2025**, *82*, 103607, doi:10.1016/j.redox.2025.103607.
172. Winterbourn, C.C. Reconciling the Chemistry and Biology of Reactive Oxygen Species. *Nat Chem Biol* **2008**, *4*, 278–286, doi:10.1038/nchembio.85.
173. Winterbourn, C.C.; Peskin, A.V.; Kleffmann, T.; Radi, R.; Pace, P.E. Carbon Dioxide/Bicarbonate Is Required for Sensitive Inactivation of Mammalian Glyceraldehyde-3-Phosphate Dehydrogenase by Hydrogen Peroxide. *Proc National Acad Sci* **2023**, *120*, e2221047120, doi:10.1073/pnas.2221047120.
174. Dickinson, B.C.; Chang, C.J. Chemistry and Biology of Reactive Oxygen Species in Signaling or Stress Responses. *Nat Chem Biol* **2011**, *7*, 504–511, doi:10.1038/nchembio.607.
175. Prigogine, I. Dissipative Structures, Dynamics and Entropy. *Int. J. Quantum Chem.* **1975**, *9*, 443–456, doi:10.1002/qua.560090854.
176. Manford, A.G.; Rodríguez-Pérez, F.; Shih, K.Y.; Shi, Z.; Berdan, C.A.; Choe, M.; Titov, D.V.; Nomura, D.K.; Rape, M. A Cellular Mechanism to Detect and Alleviate Reductive Stress. *Cell* **2020**, *183*, 46-61.e21, doi:10.1016/j.cell.2020.08.034.
177. Noguchi, N.; Saito, Y.; Niki, E. Actions of Thiols, Persulfides, and Polysulfides as Free Radical Scavenging Antioxidants. *Antioxidants Redox Signal* **2022**, *0*, doi:10.1089/ars.2022.0191.
178. Byrne, D.P.; Shrestha, S.; Galler, M.; Cao, M.; Daly, L.A.; Campbell, A.E.; Eyers, C.E.; Veal, E.A.; Kannan, N.; Eyers, P.A. Aurora A Regulation by Reversible Cysteine Oxidation Reveals Evolutionarily Conserved Redox Control of Ser/Thr Protein Kinase Activity. *Sci Signal* **2020**, *13*, eaax2713, doi:10.1126/scisignal.aax2713.
179. Kalinichenko, A.L.; Jappy, D.; Solius, G.M.; Maltsev, D.I.; Bogdanova, Y.A.; Mukhametshina, L.F.; Sokolov, R.A.; Moshchenko, A.A.; Shaydurov, V.A.; Rozov, A.V.; et al. Chemogenetic Emulation of Intraneuronal Oxidative Stress Affects Synaptic Plasticity. *Redox Biol* **2023**, *60*, 102604, doi:10.1016/j.redox.2023.102604.
180. Akter, S.; Fu, L.; Jung, Y.; Conte, M.L.; Lawson, J.R.; Lowther, W.T.; Sun, R.; Liu, K.; Yang, J.; Carroll, K.S. Chemical Proteomics Reveals New Targets of Cysteine Sulfinic Acid Reductase. *Nat Chem Biol* **2018**, *14*, 995–1004, doi:10.1038/s41589-018-0116-2.
181. Montero, L.; Okraine, Y.V.; Orlowski, J.; Matzkin, S.; Scarponi, I.; Miranda, M.V.; Nusblat, A.; Gottifredi, V.; Alonso, L.G. Conserved Cysteine-Switches for Redox Sensing Operate in the Cyclin-Dependent Kinase Inhibitor P21(CIP/KIP) Protein Family. *Free Radic. Biol. Med.* **2024**, *224*, 494–505, doi:10.1016/j.freeradbiomed.2024.09.013.
182. Mills, E.L.; Harmon, C.; Jedrychowski, M.P.; Xiao, H.; Gruszczyk, A.V.; Bradshaw, G.A.; Tran, N.; Garrity, R.; Laznik-Bogoslavski, D.; Szpyt, J.; et al. Cysteine 253 of UCP1 Regulates Energy Expenditure and Sex-Dependent Adipose Tissue Inflammation. *Cell Metab* **2021**, doi:10.1016/j.cmet.2021.11.003.
183. Ruiz, D.G.; Sandoval-Perez, A.; Rangarajan, A.V.; Gunderson, E.L.; Jacobson, M.P. Cysteine Oxidation in Proteins: Structure, Biophysics, and Simulation. *Biochemistry* **2022**, *61*, 2165–2176, doi:10.1021/acs.biochem.2c00349.

 doi:10.20944/preprints202507.2120.v1

184. Göbl, C.; Morris, V.K.; Dam, L. van; Visscher, M.; Polderman, P.E.; Hartlmüller, C.; Ruiter, H. de; Hora, M.; Liesinger, L.; Birner-Gruenberger, R.; et al. Cysteine Oxidation Triggers Amyloid Fibril Formation of the Tumor Suppressor P16INK4A. *Redox Biol* **2020**, *28*, 101316, doi:10.1016/j.redox.2019.101316.
185. Burgoyne, J.R.; Madhani, M.; Cuello, F.; Charles, R.L.; Brennan, J.P.; Schröder, E.; Browning, D.D.; Eaton, P. Cysteine Redox Sensor in PKGIa Enables Oxidant-Induced Activation. *Science* **2007**, *317*, 1393–1397, doi:10.1126/science.1144318.
186. Bodnar, Y.; Lillig, C.H. Cysteinyl and Methionyl Redox Switches: Structural Prerequisites and Consequences. *Redox Biol.* **2023**, *65*, 102832, doi:10.1016/j.redox.2023.102832.
187. Gao, J.; Newberry, M. Fractal Scaling and the Aesthetics of Trees. *arXiv* **2024**, doi:10.48550/arxiv.2402.13520.
188. Bannink, T.; Buhrman, H. Quantum Pascal's Triangle and Sierpinski's Carpet. *arXiv* **2017**, doi:10.48550/arxiv.1708.07429.
189. Harman, D. Aging: A Theory Based on Free Radical and Radiation Chemistry. *J Gerontology* **1956**, *11*, 298–300, doi:10.1093/geronj/11.3.298.
190. Harman, D. Origin and Evolution of the Free Radical Theory of Aging: A Brief Personal History, 1954–2009. *Biogerontology* **2009**, *10*, 773, doi:10.1007/s10522-009-9234-2.
191. Meo, S.D.; Venditti, P. Evolution of the Knowledge of Free Radicals and Other Oxidants. *Oxidative Med. Cell. Longev.* **2020**, *2020*, 9829176, doi:10.1155/2020/9829176.
192. Gladyshev, V.N. The Free Radical Theory of Aging Is Dead. Long Live the Damage Theory! *Antioxid. Redox Signal.* **2014**, *20*, 727–731, doi:10.1089/ars.2013.5228.
193. Finkel, T.; Holbrook, N.J. Oxidants, Oxidative Stress and the Biology of Ageing. *Nature* **2000**, *408*, 239–247, doi:10.1038/35041687.
194. Cobley, J.; Chatzinikolaou, P.N.; Schmidt, C.A. Non-Linear Cysteine Redox Proteoform Dynamics in the I-Space: A Novel Theory of Redox Regulation. **2024**, doi:10.2139/ssrn.5047335.
195. Gutteridge, J.M.C.; Halliwell, B. Antioxidants: Molecules, Medicines, and Myths. *Biochem Bioph Res Co* **2010**, *393*, 561–564, doi:10.1016/j.bbrc.2010.02.071.
196. Halliwell, B. Reflections of an Aging Free Radical. *Free Radic Biology Medicine* **2020**, *161*, 234–245, doi:10.1016/j.freeradbiomed.2020.10.010.
197. Murphy, M.P. Antioxidants as Therapies: Can We Improve on Nature? *Free Radical Bio Med* **2014**, *66*, 20–23, doi:10.1016/j.freeradbiomed.2013.04.010.
198. Frijhoff, J.; Winyard, P.G.; Zarkovic, N.; Davies, S.S.; Stocker, R.; Cheng, D.; Knight, A.R.; Taylor, E.L.; Oettrich, J.; Ruskovska, T.; et al. Clinical Relevance of Biomarkers of Oxidative Stress. *Antioxid. Redox Signal.* **2015**, *23*, 1144–1170, doi:10.1089/ars.2015.6317.
199. Williamson, J.; Hughes, C.M.; Cobley, J.N.; Davison, G.W. The Mitochondria-Targeted Antioxidant MitoQ, Attenuates Exercise-Induced Mitochondrial DNA Damage. *Redox Biol* **2020**, *36*, 101673, doi:10.1016/j.redox.2020.101673.
200. Cobley, J.N.; McHardy, H.; Morton, J.P.; Nikolaidis, M.G.; Close, G.L. Influence of Vitamin C and Vitamin E on Redox Signaling: Implications for Exercise Adaptations. *Free Radical Bio Med* **2015**, *84*, 65–76, doi:10.1016/j.freeradbiomed.2015.03.018.
201. Halliwell, B. Reactive Oxygen Species and the Central Nervous System. *J. Neurochem.* **1992**, *59*, 1609–1623, doi:10.1111/j.1471-4159.1992.tb10990.x.
202. Halliwell, B. Oxidative Stress and Neurodegeneration: Where Are We Now? *J. Neurochem.* **2006**, *97*, 1634–1658, doi:10.1111/j.1471-4159.2006.03907.x.
203. Vaccaro, A.; Dor, Y.K.; Nambara, K.; Pollina, E.A.; Lin, C.; Greenberg, M.E.; Rogulja, D. Sleep Loss Can Cause Death through Accumulation of Reactive Oxygen Species in the Gut. *Cell* **2020**, *181*, 1307-1328.e15, doi:10.1016/j.cell.2020.04.049.
204. Rorsman, H.O.; Müller, M.A.; Liu, P.Z.; Sanchez, L.G.; Kempf, A.; Gerbig, S.; Spengler, B.; Miesenböck, G. Sleep Pressure Accumulates in a Voltage-Gated Lipid Peroxidation Memory. *Nature* **2025**, *641*, 232–239, doi:10.1038/s41586-025-08734-4.
205. Kempf, A.; Song, S.M.; Talbot, C.B.; Miesenböck, G. A Potassium Channel β-Subunit Couples Mitochondrial Electron Transport to Sleep. *Nature* **2019**, *568*, 230–234, doi:10.1038/s41586-019-1034-5.

 doi:10.20944/preprints202507.2120.v1

206. Cobley, J.N.; Noble, A.; Jimenez-Fernandez, E.; Moya, M.-T.V.; Guille, M.; Husi, H. Catalyst-Free Click PEGylation Reveals Substantial Mitochondrial ATP Synthase Sub-Unit Alpha Oxidation before and after Fertilisation. *Redox Biol* **2019**, *26*, 101258, doi:10.1016/j.redox.2019.101258.
207. Tuncay, A.; Noble, A.; Guille, M.; Cobley, J.N. RedoxiFluor: A Microplate Technique to Quantify Target-Specific Protein Thiol Redox State in Relative Percentage and Molar Terms. *Free Radical Bio Med* **2022**, *181*, 118–129, doi:10.1016/j.freeradbiomed.2022.01.023.
208. Tuncay, A.; Crabtree, D.R.; Muggeridge, D.J.; Husi, H.; Cobley, J.N. Performance Benchmarking Microplate-Immunoassays for Quantifying Target-Specific Cysteine Oxidation Reveals Their Potential for Understanding Redox-Regulation and Oxidative Stress. *Free Radical Bio Med* **2023**, *204*, 252–265, doi:10.1016/j.freeradbiomed.2023.05.006.
209. Po, A.; Eyers, C.E. Top-Down Proteomics and the Challenges of True Proteoform Characterization. *J. Proteome Res.* **2023**, *22*, 3663–3675, doi:10.1021/acs.jproteome.3c00416.
210. Cao, M.; Day, A.M.; Galler, M.; Latimer, H.R.; Byrne, D.P.; Foy, T.W.; Dwyer, E.; Bennett, E.; Palmer, J.; Morgan, B.A.; et al. A Peroxiredoxin-P38 MAPK Scaffold Increases MAPK Activity by MAP3K-Independent Mechanisms. *Mol. Cell* **2023**, *83*, 3140-3154.e7, doi:10.1016/j.molcel.2023.07.018.
211. Donnelly, D.P.; Rawlins, C.M.; DeHart, C.J.; Fornelli, L.; Schachner, L.F.; Lin, Z.; Lippens, J.L.; Aluri, K.C.; Sarin, R.; Chen, B.; et al. Best Practices and Benchmarks for Intact Protein Analysis for Top-down Mass Spectrometry. *Nat. Methods* **2019**, *16*, 587–594, doi:10.1038/s41592-019-0457-0.
212. Timp, W.; Timp, G. Beyond Mass Spectrometry, the next Step in Proteomics. *Sci Adv* **2020**, *6*, eaax8978, doi:10.1126/sciadv.aax8978.
213. Siuti, N.; Kelleher, N.L. Decoding Protein Modifications Using Top-down Mass Spectrometry. *Nat. Methods* **2007**, *4*, 817–821, doi:10.1038/nmeth1097.
214. Tentori, A.M.; Yamauchi, K.A.; Herr, A.E. Detection of Isoforms Differing by a Single Charge Unit in Individual Cells. *Angewandte Chemie Int Ed* **2016**, *55*, 12431–12435, doi:10.1002/anie.201606039.
215. Brown, K.A.; Melby, J.A.; Roberts, D.S.; Ge, Y. Top-down Proteomics: Challenges, Innovations, and Applications in Basic and Clinical Research. *Expert Rev. Proteom.* **2020**, *17*, 719–733, doi:10.1080/14789450.2020.1855982.
216. Chen, B.; Brown, K.A.; Lin, Z.; Ge, Y. Top-Down Proteomics: Ready for Prime Time? *Anal Chem* **2018**, *90*, 110–127, doi:10.1021/acs.analchem.7b04747.
217. Ansong, C.; Wu, S.; Meng, D.; Liu, X.; Brewer, H.M.; Kaiser, B.L.D.; Nakayasu, E.S.; Cort, J.R.; Pevzner, P.; Smith, R.D.; et al. Top-down Proteomics Reveals a Unique Protein S-Thiolation Switch in Salmonella Typhimurium in Response to Infection-like Conditions. *Proc National Acad Sci* **2013**, *110*, 10153–10158, doi:10.1073/pnas.1221210110.
218. Kelleher, N.L.; Lin, H.Y.; Valaskovic, G.A.; Aaserud, D.J.; Fridriksson, E.K.; McLafferty, F.W. Top Down versus Bottom Up Protein Characterization by Tandem High-Resolution Mass Spectrometry. *J. Am. Chem. Soc.* **1999**, *121*, 806–812, doi:10.1021/ja973655h.
219. Azzi, A. Oxidative Stress: What Is It? Can It Be Measured? Where Is It Located? Can It Be Good or Bad? Can It Be Prevented? Can It Be Cured? *Antioxidants* **2022**, *11*, 1431, doi:10.3390/antiox11081431.
220. Noble, A.; Guille, M.; Cobley, J.N. ALISA: A Microplate Assay to Measure Protein Thiol Redox State. *Free Radical Bio Med* **2021**, *174*, 272–280, doi:10.1016/j.freeradbiomed.2021.08.018.
221. Muggeridge, D.J.; Crabtree, D.R.; Tuncay, A.; Megson, I.L.; Davison, G.; Cobley, J.N. Exercise Decreases PP2A-Specific Reversible Thiol Oxidation in Human Erythrocytes: Implications for Redox Biomarkers. *Free Radical Bio Med* **2022**, *182*, 73–78, doi:10.1016/j.freeradbiomed.2022.02.019.
222. Kramer, P.A.; Duan, J.; Gaffrey, M.J.; Shukla, A.K.; Wang, L.; Bammler, T.K.; Qian, W.-J.; Marcinek, D.J. Fatiguing Contractions Increase Protein S-Glutathionylation Occupancy in Mouse Skeletal Muscle. *Redox Biol.* **2018**, *17*, 367–376, doi:10.1016/j.redox.2018.05.011.
223. Davies, K.J.A. Adaptive Homeostasis. *Mol. Asp. Med.* **2016**, *49*, 1–7, doi:10.1016/j.mam.2016.04.007.
224. Ostrom, E.L.; Traustadóttir, T. Aerobic Exercise Training Partially Reverses the Impairment of Nrf2 Activation in Older Humans. *Free Radic. Biol. Med.* **2020**, *160*, 418–432, doi:10.1016/j.freeradbiomed.2020.08.016.

 doi:10.20944/preprints202507.2120.v1

225. Henriquez-Olguin, C.; Meneses-Valdes, R.; Jensen, T.E. Compartmentalized Muscle Redox Signals Controlling Exercise Metabolism – Current State, Future Challenges. *Redox Biol* **2020**, *35*, 101473, doi:10.1016/j.redox.2020.101473.
226. Henríquez-Olguin, C.; Knudsen, J.R.; Raun, S.H.; Li, Z.; Dalbram, E.; Treebak, J.T.; Sylow, L.; Holmdahl, R.; Richter, E.A.; Jaimovich, E.; et al. Cytosolic ROS Production by NADPH Oxidase 2 Regulates Muscle Glucose Uptake during Exercise. *Nat Commun* **2019**, *10*, 4623, doi:10.1038/s41467-019-12523-9.
227. Henriquez-Olguin, C.; Meneses-Valdes, R.; Kritsiligkou, P.; Fuentes-Lemus, E. From Workout to Molecular Switches: How Does Skeletal Muscle Produce, Sense, and Transduce Subcellular Redox Signals? *Free Radic. Biol. Med.* **2023**, *209*, 355–365, doi:10.1016/j.freeradbiomed.2023.10.404.
228. Margaritelis, N.V. Personalized Redox Biology: Designs and Concepts. *Free Radic. Biol. Med.* **2023**, *208*, 112–125, doi:10.1016/j.freeradbiomed.2023.08.003.
229. Xia, Q.; Casas-Martinez, J.C.; Zarzuela, E.; Muñoz, J.; Miranda-Vizuete, A.; Goljanek-Whysall, K.; McDonagh, B. Peroxiredoxin 2 Is Required for the Redox Mediated Adaptation to Exercise. *Redox Biol* **2023**, *60*, 102631, doi:10.1016/j.redox.2023.102631.
230. Margaritelis, N.V.; Kyparos, A.; Paschalis, V.; Theodorou, A.A.; Panayiotou, G.; Zafeiridis, A.; Dipla, K.; Nikolaidis, M.G.; Vrabas, I.S. Reductive Stress after Exercise: The Issue of Redox Individuality. *Redox Biol.* **2014**, *2*, 520–528, doi:10.1016/j.redox.2014.02.003.
231. Goulev, Y.; Morlot, S.; Matifas, A.; Huang, B.; Molin, M.; Toledano, M.B.; Charvin, G. Nonlinear Feedback Drives Homeostatic Plasticity in H2O2 Stress Response. *eLife* **2017**, *6*, e23971, doi:10.7554/elife.23971.
232. Pillay, C.S.; Rohwer, J.M. Computational Models as Catalysts for Investigating Redoxin Systems. *Essays Biochem.* **2024**, doi:10.1042/ebc20230036.
233. Huang, B.K.; Sikes, H.D. Quantifying Intracellular Hydrogen Peroxide Perturbations in Terms of Concentration. *Redox Biol* **2014**, *2*, 955–962, doi:10.1016/j.redox.2014.08.001.
234. Ammar, C.; Schessner, J.P.; Willems, S.; Michaelis, A.C.; Mann, M. Accurate Label-Free Quantification by DirectLFQ to Compare Unlimited Numbers of Proteomes. *Mol. Cell. Proteom.* **2023**, *22*, 100581, doi:10.1016/j.mcpro.2023.100581.
235. Picotti, P.; Aebersold, R. Selected Reaction Monitoring–Based Proteomics: Workflows, Potential, Pitfalls and Future Directions. *Nat Methods* **2012**, *9*, 555–566, doi:10.1038/nmeth.2015.
236. Burniston, J.G.; Kenyani, J.; Gray, D.; Guadagnin, E.; Jarman, I.H.; Cobley, J.N.; Cuthbertson, D.J.; Chen, Y.-W.; Wastling, J.M.; Lisboa, P.J.; et al. Conditional Independence Mapping of DIGE Data Reveals PDIA3 Protein Species as Key Nodes Associated with Muscle Aerobic Capacity. *J Proteomics* **2014**, *106*, 230–245, doi:10.1016/j.jprot.2014.04.015.
237. Malik, Z.A.; Cobley, J.N.; Morton, J.P.; Close, G.L.; Edwards, B.J.; Koch, L.G.; Britton, S.L.; Burniston, J.G. Label-Free LC-MS Profiling of Skeletal Muscle Reveals Heart-Type Fatty Acid Binding Protein as a Candidate Biomarker of Aerobic Capacity. *Proteomes* **2013**, *1*, 290–308, doi:10.3390/proteomes1030290.
238. Cobley, J.N.; Malik, Z.Ab.; Morton, J.P.; Close, G.L.; Edwards, B.J.; Burniston, J.G. Age- and Activity-Related Differences in the Abundance of Myosin Essential and Regulatory Light Chains in Human Muscle. *Proteomes* **2016**, *4*, 15, doi:10.3390/proteomes4020015.
239. Burger, N.; Mittenbühler, M.J.; Xiao, H.; Shin, S.; Wei, S.M.; Henze, E.K.; Schindler, S.; Mehravar, S.; Wood, D.M.; Petrocelli, J.J.; et al. The Human Zinc-Binding Cysteine Proteome. *Cell* **2025**, *188*, 832-850.e27, doi:10.1016/j.cell.2024.11.025.
240. Backus, K.M.; Correia, B.E.; Lum, K.M.; Forli, S.; Horning, B.D.; González-Páez, G.E.; Chatterjee, S.; Lanning, B.R.; Teijaro, J.R.; Olson, A.J.; et al. Proteome-Wide Covalent Ligand Discovery in Native Biological Systems. *Nature* **2016**, *534*, 570–574, doi:10.1038/nature18002.
241. Weerapana, E.; Wang, C.; Simon, G.M.; Richter, F.; Khare, S.; Dillon, M.B.D.; Bachovchin, D.A.; Mowen, K.; Baker, D.; Cravatt, B.F. Quantitative Reactivity Profiling Predicts Functional Cysteines in Proteomes. *Nature* **2010**, *468*, 790–795, doi:10.1038/nature09472.
242. Cravatt, B.F.; Simon, G.M.; III, J.R.Y. The Biological Impact of Mass-Spectrometry-Based Proteomics. *Nature* **2007**, *450*, 991–1000, doi:10.1038/nature06525.
243. Kemper, E.K.; Zhang, Y.; Dix, M.M.; Cravatt, B.F. Global Profiling of Phosphorylation-Dependent Changes in Cysteine Reactivity. *Nat Methods* **2022**, *19*, 341–352, doi:10.1038/s41592-022-01398-2.

 doi:10.20944/preprints202507.2120.v1

244. Suskiewicz, M.J. The Logic of Protein Post-translational Modifications (PTMs): Chemistry, Mechanisms and Evolution of Protein Regulation through Covalent Attachments. *BioEssays* **2024**, *46*, e2300178, doi:10.1002/bies.202300178.
245. Lancaster, N.M.; Sinitcyn, P.; Forny, P.; Peters-Clarke, T.M.; Fecher, C.; Smith, A.J.; Shishkova, E.; Arrey, T.N.; Pashkova, A.; Robinson, M.L.; et al. Fast and Deep Phosphoproteome Analysis with the Orbitrap Astral Mass Spectrometer. *Nat. Commun.* **2024**, *15*, 7016, doi:10.1038/s41467-024-51274-0.
246. Davies, M.J. Methionine Oxidation Products as Biomarkers of Oxidative Damage to Proteins and Modulators of Cellular Metabolism and Toxicity. *Redox Biochem. Chem.* **2025**, *12*, 100052, doi:10.1016/j.rbc.2025.100052.
247. Davies, M.J. Protein Oxidation and Peroxidation. *Biochem J* **2016**, *473*, 805–825, doi:10.1042/bj20151227.
248. He, D.; Feng, H.; Sundberg, B.; Yang, J.; Powers, J.; Christian, A.H.; Wilkinson, J.E.; Monnin, C.; Avizonis, D.; Thomas, C.J.; et al. Methionine Oxidation Activates Pyruvate Kinase M2 to Promote Pancreatic Cancer Metastasis. *Mol Cell* **2022**, *82*, 3045-3060.e11, doi:10.1016/j.molcel.2022.06.005.
249. Lin, S.; Yang, X.; Jia, S.; Weeks, A.M.; Hornsby, M.; Lee, P.S.; Nichiporuk, R.V.; Iavarone, A.T.; Wells, J.A.; Toste, F.D.; et al. Redox-Based Reagents for Chemoselective Methionine Bioconjugation. *Science* **2017**, *355*, 597–602, doi:10.1126/science.aal3316.
250. Bartesaghi, S.; Radi, R. Fundamentals on the Biochemistry of Peroxynitrite and Protein Tyrosine Nitration. *Redox Biol.* **2018**, *14*, 618–625, doi:10.1016/j.redox.2017.09.009.
251. Radi, R. Interplay of Carbon Dioxide and Peroxide Metabolism in Mammalian Cells. *J Biol Chem* **2022**, 102358, doi:10.1016/j.jbc.2022.102358.
252. Radi, R. Oxygen Radicals, Nitric Oxide, and Peroxynitrite: Redox Pathways in Molecular Medicine. *Proc National Acad Sci* **2018**, *115*, 5839–5848, doi:10.1073/pnas.1804932115.
253. Sultana, R.; Butterfield, D.A. Identification of the Oxidative Stress Proteome in the Brain. *Free Radic. Biol. Med.* **2011**, *50*, 487–494, doi:10.1016/j.freeradbiomed.2010.11.021.
254. Butterfield, D.A.; Halliwell, B. Oxidative Stress, Dysfunctional Glucose Metabolism and Alzheimer Disease. *Nat Rev Neurosci* **2019**, *20*, 148–160, doi:10.1038/s41583-019-0132-6.
255. Sultana, R.; Butterfield, D.A. Oxidative Modification of Brain Proteins in Alzheimer's Disease: Perspective on Future Studies Based on Results of Redox Proteomics Studies. *J. Alzheimer's Dis.* **2013**, *33*, S243–S251, doi:10.3233/jad-2012-129018.
256. Bettinger, J.Q.; Simon, M.; Korotkov, A.; Welle, K.A.; Hryhorenko, J.R.; Seluanov, A.; Gorbunova, V.; Ghaemmaghami, S. Accurate Proteomewide Measurement of Methionine Oxidation in Aging Mouse Brains. *J. Proteome Res.* **2022**, *21*, 1495–1509, doi:10.1021/acs.jproteome.2c00127.
257. Aledo, J.C.; Aledo, P. Susceptibility of Protein Methionine Oxidation in Response to Hydrogen Peroxide Treatment–Ex Vivo versus In Vitro: A Computational Insight. *Antioxidants* **2020**, *9*, 987, doi:10.3390/antiox9100987.
258. Dai, C.; Pfeuffer, J.; Wang, H.; Zheng, P.; Käll, L.; Sachsenberg, T.; Demichev, V.; Bai, M.; Kohlbacher, O.; Perez-Riverol, Y. Quantms: A Cloud-Based Pipeline for Quantitative Proteomics Enables the Reanalysis of Public Proteomics Data. *Nat. Methods* **2024**, *21*, 1603–1607, doi:10.1038/s41592-024-02343-1.